AD_____

Award Number: DAMD17-00-1-0081

TITLE: Targeting of Prostate Cancer with Hyaluronan-Binding Proteins

PRINCIPAL INVESTIGATOR: Lurong Zhang, M.D., Ph.D.

CONTRACTING ORGANIZATION: Georgetown University Medical Center
Washington, DC 20007

REPORT DATE: June 2001

TYPE OF REPORT: Annual

PREPARED FOR: U.S. Army Medical Research and Materiel Command
Fort Detrick, Maryland 21702-5012

DISTRIBUTION STATEMENT: Approved for Public Release;
Distribution Unlimited

REPORT DOCUMENTATION PAGE

Form Approved
OMB No. 074-0188

1. AGENCY USE ONLY (Leave blank)	2. REPORT DATE	3. REPORT TYPE AND DATES COVERED
	June 2001	Annual (1 Jun 00 - 31 May 01)

4. TITLE AND SUBTITLE
Targeting of Prostate Cancer with Hyaluronan-Binding Proteins

5. FUNDING NUMBERS
DAMD17-00-1-0081

6. AUTHOR(S)
Lurong Zhang, M.D., Ph.D.

7. PERFORMING ORGANIZATION NAME(S) AND ADDRESS(ES)
Georgetown University Medical Center
Washington, DC 20007

E-Mail: zhangl@georgetown.edu

8. PERFORMING ORGANIZATION REPORT NUMBER

9. SPONSORING / MONITORING AGENCY NAME(S) AND ADDRESS(ES)
U.S. Army Medical Research and Materiel Command
Fort Detrick, Maryland 21702-5012

10. SPONSORING / MONITORING AGENCY REPORT NUMBER

11. SUPPLEMENTARY NOTES
This report contains colored photos

12a. DISTRIBUTION / AVAILABILITY STATEMENT
Approved for Public Release; Distribution Unlimited

12b. DISTRIBUTION CODE

13. ABSTRACT *(Maximum 200 Words)*

This study is to test if hyaluronan (HA) binding proteins (HABP), an abundant protein in cartilage, is a new category of anti-tumor substance. This hypothesis is based on the facts that: **1)** the shake cartilage powder or its extracts have been widely used by patients with different tumors in USA, Europe and Asia for a decade, in believing that avasscular cartilage might contain some natural anti-tumor/angiogenesis substance; **2)** certain angiogenic inhibitor, such as endostatin, has HA binding domain; and **3)** some hyaluronan binding proteins, such as soluble CD44 and proteins from scapular chondrocytes or have anti-tumor/angiogenesis effect.

In the past year, we have purified a large quantity of hyaluronan binding proteins from bovine cartilage and test its anti-tumor and anti-angiogenesis effects. The result are promising, indicating that **1)** HABP can inhibit the anchorage-dependent and independent growth of tumor cells; **2)** HABP can inhibit proliferation and migration of endothelial cells *in vitro* and angiogenesis *in vivo*; **3)** HABP can reduce the growth of TSU prostate cancer and other tumor *in vivo*; **4)** HABP can inhibit the experimental lung metastasis. It seems that HABP is a good candidate for development into a new anti-tumor agent. Next year, we will focus on test HABP from human source using molecular biology approaches. The human HABP will be cloned, inserted into expression vector and transfected into prostate cancer cells or infected in established prostate tumor to see the effect of human HABP on tumor growth. The underlying molecular mechanism of HABP by which it exerts anti-tumor/angiogenesis effect will also be explored.

14. SUBJECT TERMS	15. NUMBER OF PAGES
Hyaluronan-Binding Proteins, Experimental Therapy, Prostate Cancer, Angiogenesis	32
	16. PRICE CODE

17. SECURITY CLASSIFICATION OF REPORT	18. SECURITY CLASSIFICATION OF THIS PAGE	19. SECURITY CLASSIFICATION OF ABSTRACT	20. LIMITATION OF ABSTRACT
Unclassified	Unclassified	Unclassified	Unlimited

Table of Contents

INTRODUCTION

Although much progress has been made in elucidating the underlying molecular mechanisms responsible for prostate cancer in recent years, effective treatments for this disease have not progressed at the same pace. New therapeutic approaches are badly needed.

In last decade, it has been found that some hyaluronan (HA, a major component of extracellular metrix) binding proteins, such as soluble CD44 and proteins from scapular chondrocytes or cartilage have anti-tumor or anti-angiogenesis effect (1-4). In addition, some angiogenic inhibitors, such as endostatin, have HA binding domain demonstrated by crystal structure (5-7). Furthermore, the shake cartilage powder or its extracts have been on the shelf of health food market in USA (FDA IND# 43 033, approved on Fab 7, 1994), Europe and Asia for a decade. This substance has been widely used by patients with different tumors, in believing that avasscular cartilage might contain some natural anti-angiogenesis substance. Indeed, this substance has exhibit anti-cancer effect in some patients, which might be associated with that some components of shark cartilage escape digestion, and enter tumor sites via the blood circulation. Although the therapeutic value of shake cartilage for cancer is still controversial, Alternative Medicine Center in National Institute of Health has made decision to test the efficacy of this substance (8-21). The cartilage contains an abundance of HA binding proteins (HABP, 22-25). Whether the anti-tumor/angiogenesis effect of shark cartilage achieved in a proportion of cancer patients is due to a small amount of HABP passing through impaired mucous of gastro-intestine remains to be investigated.

Based on others and our preliminary data, we hypothesize that HABP may be a new anti-tumor substance.

To test our hypothesis, we used HA-Sepharose 4 B affinity column to purify a large quantity of HABP from bovine cartilage, and test its anti-tumor/metastasis/angiogenesis effect *in vitro* and *in vivo*. The results show that: **1)** HABP can inhibit the anchorage-dependent and independent growth of tumor cells; **2)** HABP can inhibit proliferation and migration of endothelial cells *in vitro* and angiogenesis *in vivo*; **3)** HABP can reduce the growth of TSU prostate cancer and other tumor *in vivo*; **4)** HABP can inhibit the experimental metastasis.

Our data suggest that HABP is likely to be a good candidate for development into a new anti-tumor agent.

Next year, we will focus on test HABP from human source using molecular biology approaches. The human HABP will be cloned, inserted into expression vector and transfected into prostate cancer cells or infected in established prostate tumor to see the effect of human HABP on tumor growth. The underlying molecular mechanism of HABP by which it exerts anti-tumor/angiogenesis effect will also be explored.

BODY

This project is to determine if HABP is an anti-tumor/angiogenesis agent. The following studies have been performed in past year.

1. To purify a large quantity of HABP from bovine cartilage:

The cartilage is a tissue that enriches in HA and HA binding proteins (HABP, 22-25). First, we wanted to see if we could purify shark cartilage HABP using our HA affinity column, since we speculated that the HABP might be the responsible molecule for the anti-tumor/angiogenesis effect that had be achieved in some cancer patients (8-21). The fresh shark cartilage was purchased from seafood market and sliced into small pieces. The purification procedure was performed according to Dr. Tengblad's method (26-27) with some modification outlined as following. The result (**Fig. 1**) showed that the shark cartilage did contain HABP that can be purified using our HA affinity column, indicating that there is a possibility of HABP in shark cartilage being the responsible molecule for anti-tumor/angiogenesis effect of shark cartilage.

Purification of HABP

Small piece of fresh cartilage
↓
4M GuHCl, 0.5M NaAc, pH5.8 to extract HABP
↓
Dialyzed against PBS
↓
Digested with Trypsin
↓
Dialyzed against 4M GuHCl
↓
HA affinity column
↓
Dialyzed against PBS
↓
Washed out unbound miscellaneous proteins with linear gradient NaCl from 1 M to 3 M
↓
Eluted HABP with 4M GuHCl
↓
Dialyzed against PBS and filtered for use

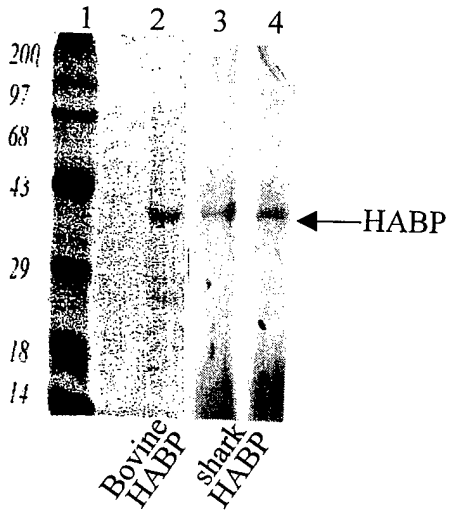

Fig. 1. Purified HABP from bovine cartilage and shark cartilage. **Lane1**: molecular markers; **Lane 2**: purified bovine HABP; **Lane 3 and 4**: purified shark HABP.

At this stage, we wanted to obtain enough HABP to test its anti-tumor/angiogenesis effect *in vitro* and *in vivo*. The fresh shark cartilage is not easy to be obtained for us, however, there is a good commercial source for bovine nasal cartilage. We had purchased a large quantity of bovine cartilage and spent 3 months to purify a large amount of bovine HABP. During the purification process, every effort was made to avoid the bacterial contamination. At the end, the endotoxin in each preparation was tested and the results was less then 5EU/ml, indicating that the purified bovine HABP could be used for both in vitro and in vivo studies.

2. To examine the effect of HABP on anchorage-dependent and independent growth of tumor cells.

To test if purified bovine HABP had its bio-activity, we first performed the anchorage-dependent and independent growth assay in tumor cells. The different amounts of HABP (5, 50 μg/ml) were added to the media of tumor cells cultured in 24 well plate, at different time points (day 2, 4, 6 and 8), the cells were harvested with 10 mM EDTA and the number was counted with Coulter Counter. The result (**Fig. 2A**) showed that the HABP inhibited the growth of tumor cells in a dose dependent manner. This inhibitory effect could be abolished by the heat-inactivation, indicating that the natural structure of this protein is essential for its activity of anti-tumor cell growth. Furthermore, the when HABP was added to the media of tumor cells that grew on soft agar, the ability of tumor cells to form colony was greatly reduced compared to the media alone control (**Fig. 2B**). These data strongly suggest that HABP could inhibit the growth of tumor cells in both anchorage-dependent and independent conditions.

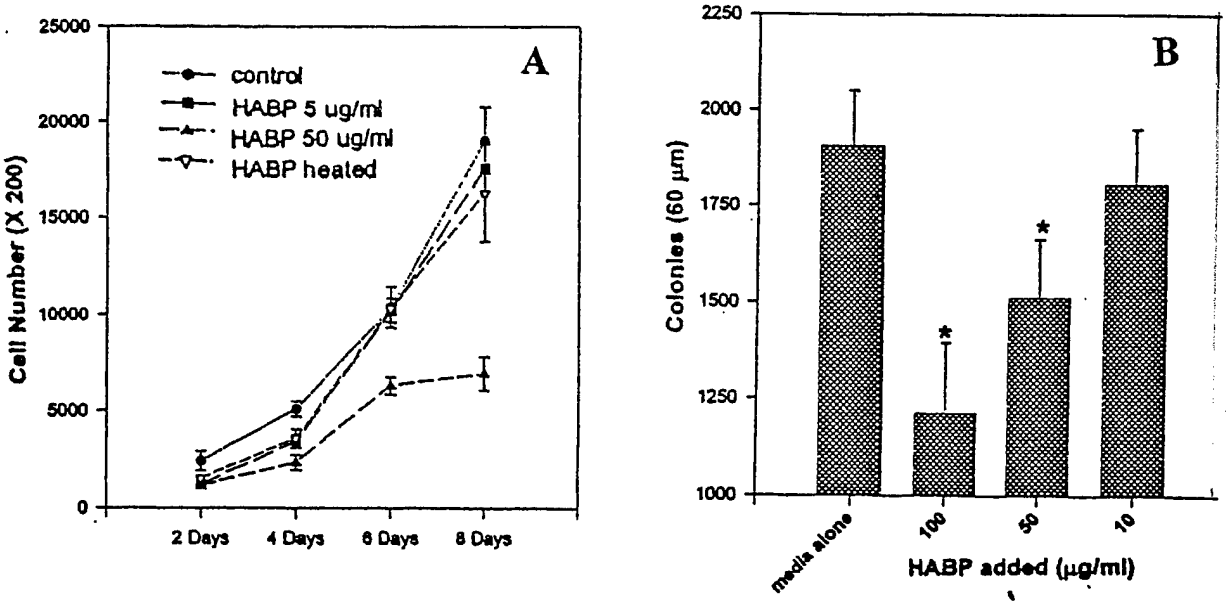

Fig. 2. Effects of bovine HABP on the growth of tumor cells. **A**: Anchorage dependent growth was inhibited by HABP; **B**: Colony formation of tumor cells was inhibited by HABP.

***3.* To examine the effect of HABP on proliferation and migration of endothelial cells *in vitro* and angiogenesis *in vivo*.**

It has been reported that cartilage contains anti-angiogenesis substance that is in part responsible for the anti-tumor effect (1-4, 8-21). To test if our purified cartilage HABP had any effect on endothelial cells, we performed in vitro and in vivo studies.

First, the different amounts of HABP (5, 50 μg/ml) or heat-inactive HABP or HABP pre-incubated with excess of HA or HA alone (as control) were added to the media of endothelial cells cultured in 24 well plate. On day 2, 4, 6 and 8, the cells were harvested with 10 mM EDTA and the number was counted with Coulter Counter. The result (**Fig. 3A**) showed that the HABP inhibited the growth of endothelial cells in a dose-dependent manner. This effect was abolished when HABP was heat-inactivated or pre-incubated with HA, indicating that the natural structure and the HA binding site are critical for its function of anti-endothelial cells.

Secondly, the HABP effect on the migration of endothelial cells was carried out with Boyden Chamber Assay. Aliquots containing 5 x 10^3 bovine retinal endothelial cells (BREC) in 50 μl media was added to bottom wells of a 48 well Boyden chamber and then covered with a Nucleopore membrane (5 μm pore size) coated with 0.1 mg/ml gelatin. The chamber was assembled and inverted for 2 hours to allow the cells to adhere to the bottom side of membrane and then turned upright. Fifty μl of 50 μg/ml of HABP (as

test) or heat-inactivated HABP was added to top wells of chamber and incubated for another 2 hours. Then, the cells on bottom side of the membrane will be carefully wiped off and the cells that have migrated to the top side of the membrane will be stained with Hema 3. The number of cells in 10 random fields will be counted. The result showed that the migration of BREC was greatly inhibited by HABP compared to the heat-inactivated HABP (**Fig. 3B and C**) and the difference was statistically significant (**Fig. 3D**).

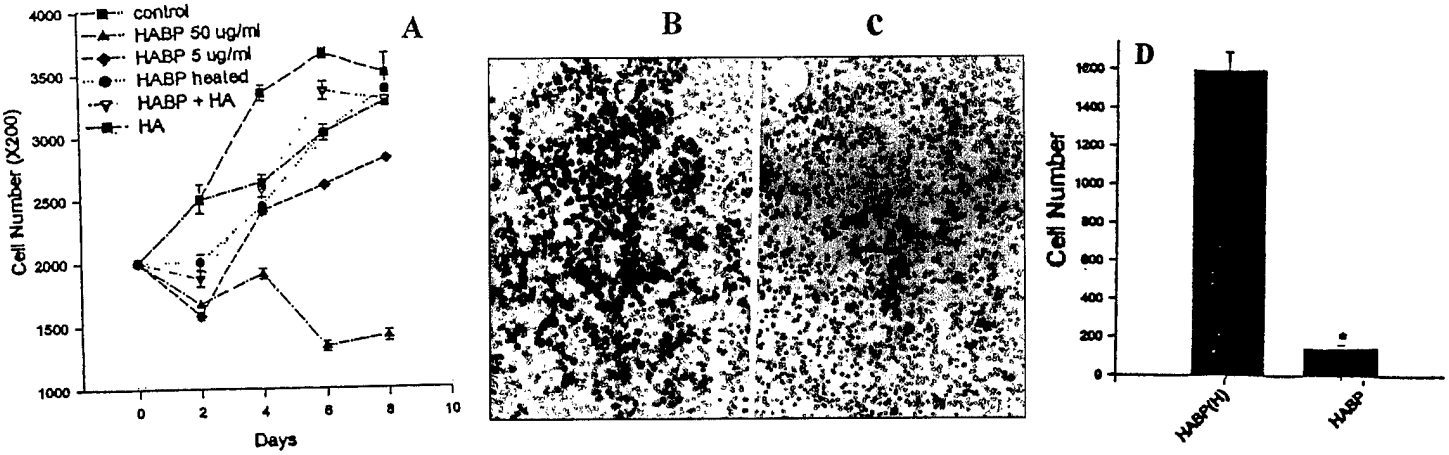

Fig. 3. Effects of bovine HABP on the growth and migration of BREC endothelial cells. **A**: Growth of BREC cells was inhibited by HABP; **B** and **C**: Boyden Chamber Assay: Migration of BREC cells treated with heat-inactivated HABP (as control, **B**) or HABP (as test, **C**). The difference was statistically significant (**D**).

Then, the effect of HABP on in vivo angiogenesis was tested in CAM (chorioallantoic membranes). Filter disks (0.5 cm in diameter) containing 15 ng of VEGF (as stimulator) will be placed on the CAMs of 6 days-old chicken embryo (10 eggs/group). 80 μg/ml of HABP (as test) or heat-inactivated HABP or saline (as controls) was administrated i.v. into the CAM once. On day 4, the filter disks were cut out and fixed in 3.7% formaldehyde. The blood vessels on the filter disks were digitally photographed and analyzed with *Optimas 5* program to determine the total vessel length. The result was expressed as vessel length index: total length of each sample/ total area measured. Indeed, the VEGF stimulated angiogenesis was inhibited by HABP (**Fig. 4B**) compared to the groups treated with heat-inactivated HABP (**Fig. 4C**) or saline (**Fig. 4A**). The difference in vessel length index among these groups was statistically significant (**Fig. 4D**).

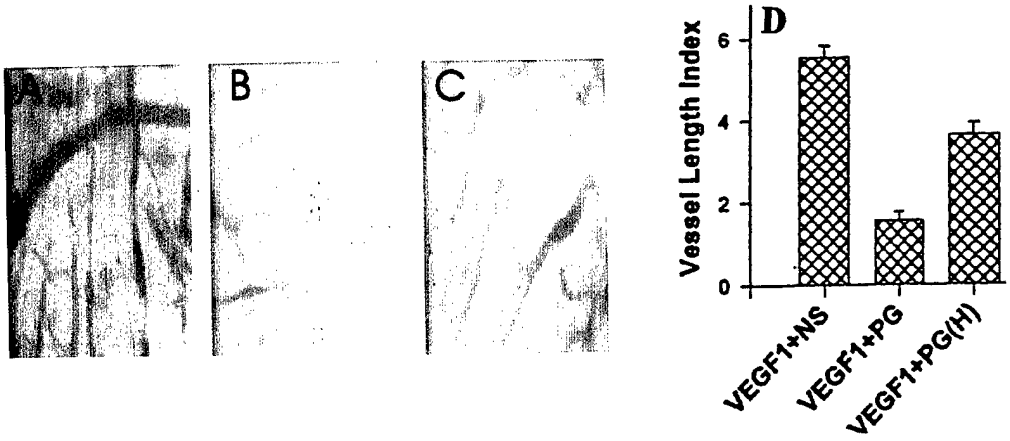

Fig. 4. Bovine HABP inhibits angiogenesis in the chicken CAM. A disc of filter paper containing 15 ng of recombinant VEGF was placed on the CAM of 8 day-old chicken embryos, and then 80 μg of HABP or saline or heat-inactivated HABP was injected i.v. Three days later, the CAMs associated with the filters were harvested and digitally photographed. The vessel length was analyzed by an *Optimas 5* program. **A**: Saline control; **B**: HABP; **C**: Heat-inactivated HABP; **D**: Analysis of vessel length.

4. To examine the effect of HABP on the growth of TSU prostate cancer and other tumor *in vivo.*

The inhibition of the growth and migration of tumor cells or endothelial cells *in vitro* suggests that HABP is likely to have effect on tumor growth *in vivo*. To test this possibility, we carried *in vivo* studies. The tumor-CAM system was used, since this was a quick, easy and cheap system (28). Furthermore, in our experience, the results from the tumor-CAM system are comparable with those obtained from the mice model system. Two million TSU or B16 tumor cells were placed on the CAMs of 10 days old chicken embryo (12 eggs/group) and allowed to grow for two day. When the established tumors could be seen by eye, 80 μg (in 200 μl saline) of HABP was iv. injected once into CAM. Four days later, the tumors were harvested, weighted and photographed. As shown in **Fig. 5A**, the tumors in treated with HABP were smaller than those treated with vehicle alone or heat-inactivated HABP, and the difference was statistically significant (**Fig. 5C and D**). The effect was dose-dependent and required a native, active form of HABP. However, there was no difference in the chicken weight (data not shown), indicating that the HABP was not toxic and did not interrupt the normal development.

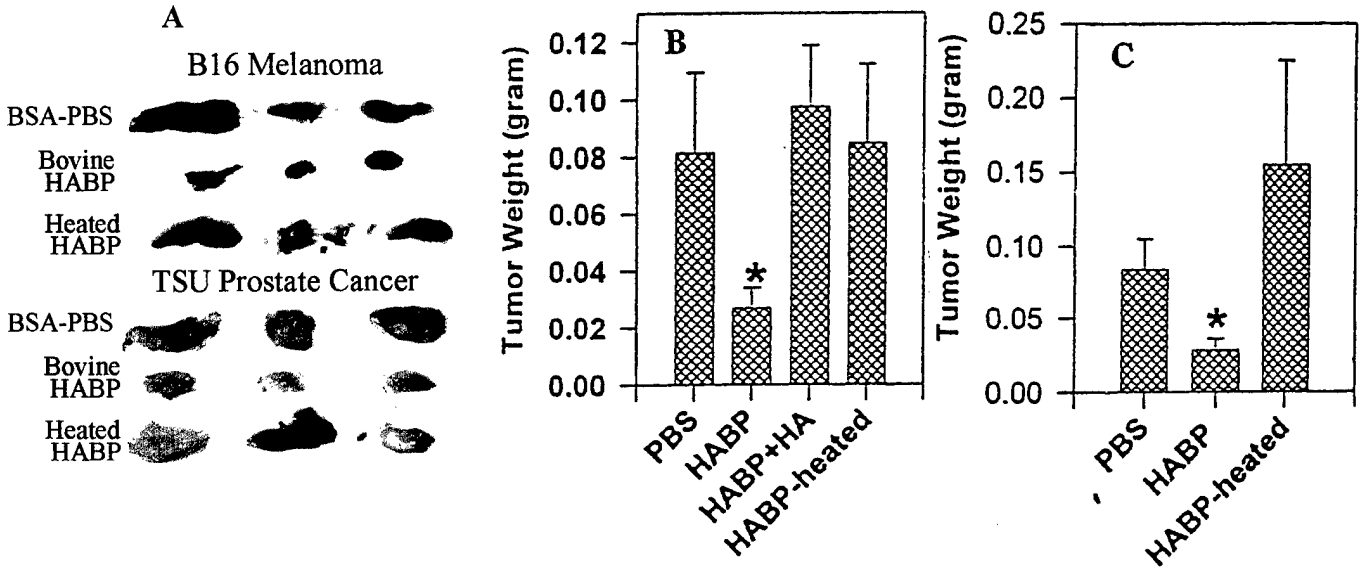

Fig 5. Bovine HABP inhibited the growth of tumors formed by TSU (top panel) and B16 (bottom panel) cells in the chicken CAM. Two million tumor cells were inoculated on the top of the CAMs and two days later, 80 μg of HABP or heat-inactivated HABP was i.v. injected once. Four days later, the tumors were harvested, photographed and weighted. **A**: Pictures of tumors; **C**: Tumor weights in TSU groups; **D**: Tumor weights in B16 groups.

5. To examine the effect of HABP on the experimental metastasis

Since the cause of death in cancer patients is mainly due to the metastasis, we were interested to see the effect of HABP on tumor metastasis. In the pilot study, we used B16 or Lewis lung metastasis models, since they are well-recognized and reliable metastasis models. Fifty thousand tumor cells were i.v. injected via tail vein into C57BL/6 syngenic mice and allowed to establish for two days. Then, the mice were treated with i.p. injection of different doses of HABP (as test) or BSA (as non-specific protein control) or HABP preincubated with excess HA. As shown in **Fig. 6A,** the experimental lung metastases formed by B16 or Lewis lung cancer cells were dramatically inhibited by i.v. injection of HABP every other day at a doses of 15 to 50 μg (**Fig. 6 B**). Importantly, in a side by side comparison study, HABP seems more effective than angiostatin, a well-known angiogenic inhibitor (**Fig. 6C**). This interesting phenomenon needs to be further confirmed and investigated.

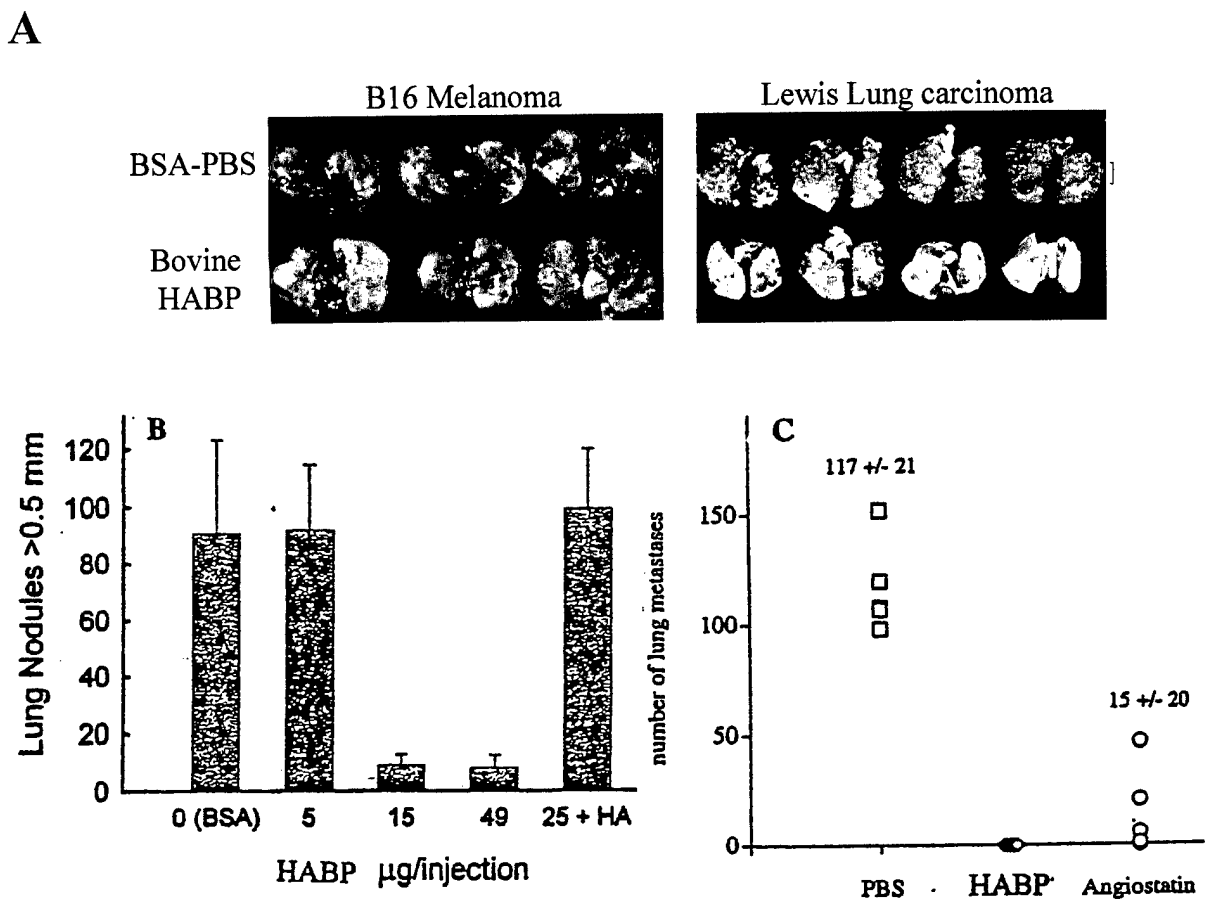

Fig 6. Bovine HABP inhibited experimental lung metastasis of B16 melanoma and Lewis Lung carcinoma. Fifty thousand B16 or Lewis lung carcinoma cells were injected into C57BL/6 mice via tail vein. After being established for two days, the mice were given i.p. injections of HABP with different concentrations of bovine HABP, HABP pre-incubated HA or 50 µg of bovine albumin (BSA) as control every other day. Two weeks later, the lungs were harvested and tumor nodules bigger than 0.5 mm were counted under a dissecting microscope. **A**: Pictures of lung metastases; **B**: Counts of lung metastatic nodules; **C**: Comparison of effect of HABP with angiostatin.

Key Research Accomplishments

Taken together, this study yielded a promising results, indicating that: **1)** HABP can be purified in a large quantity with little endotoxin contamination; **2)** HABP can inhibit the anchorage-dependent and independent growth of tumor cells; **3)** HABP can inhibit proliferation and migration of endothelial cells *in vitro* and angiogenesis *in vivo*; **4)** HABP can reduce the growth of TSU prostate cancer and other tumor *in vivo*; **5)** HABP can inhibit the experimental metastasis.

Our next studies will be focused on: **1)** using molecular biology method to obtain cDNAs of human HABP, such as link protein or aggrecan, from human cartilage cells, insert into expression vector and transfect into prostate cancer cells or infected in established prostate tumor to see the effect of human HABP on growth of human prostate cancer; **2)** alternatively, we will express the aggrecan or link protein in yeast, purify the proteins and directly test the protein in vitro and in vivo to see their effects on primary and metastatic prostate cancer; **3)** testing the anti-angiogenesis effect of human form HABPs; **4)** exploring the underlying molecular mechanism of HABP by which it exerts anti-tumor/angiogenesis effect.

Conclusions

Scientific conclusion to date:

- The purification data indicate that the HA-Sepharose 4B affinity column is a good method to purify bio-active form of HABP with little endotoxin contamination.
- Bovine HABP can inhibit the anchorage-dependent and independent growth of tumor cells.
- Bovine HABP can inhibit proliferation and migration of endothelial cells *in vitro* and angiogenesis *in vivo.*
- Bovine HABP can reduce the growth of TSU prostate cancer and other tumor *in vivo.*
- Bovine HABP can inhibit the experimental metastasis.

Reportable outcomes

Publications:

Ningfei Liu, Charles B. Underhill, Randall Lapevich, Zeqiu Han, Feng Gao, Lurong Zhang and Shawn Green: Metastatin: A hyaluronan binding complex from cartilage inhibits tumor growth. Cancer Res. 2001; 61:1022-1028

Yixin Chen, XueMing Xu, Shuigen Hong, Jinguo Chen, Ningfei Liu, Charles B. Underhill, Karen Creswell and Lurong Zhang: RGD-Tachyplesin inhibits tumor growth. Cancer Res. 2001; 61: 2434-2438

Underhill, C. B. and Lurong Zhang (2000) Analysis of hyaluronan using biotinylated hyaluronan binding proteins. Methods in Molecular Biol. 137: 441-447

References

1. Moses, M A, Sudhalter, J., and Langer, R.: Identification of an inhibitor of neovascularization from cartilage. Science 1990; 248: 1408-1410
2. Moses, M A, Sudhalter, J., and Langer, R.: Isolation and characterization of an inhibitor of neovascularization from scapular chondrocytes. J. Cell Biol. 1992: 119 (2):473-482
3. Sy, M-S., Guo, Y. J., and Stamenkovic, I.: Inhibition of tumor growth in vivo with a soluble CD44-immunoglobulin fusion protein. J. Exp. Med. 1992; 176: 623-627
4. Langer R. Brem H. Falterman K. Klein M. Folkman J. Isolations of a cartilage factor that inhibits tumor neovascularization. Science; 1976. 193(4247):70-2
5. O'Reilly MS. Boehm T. Shing Y. Fukai N. Vasios G. Lane WS. Flynn E. Birkhead JR. Olsen BR. Folkman J.: Endostatin: an endogenous inhibitor of angiogenesis and tumor growth. Cell 1997; 88(2):277-85
6. Sasaki T. Fukai N. Mann K. Gohring W. Olsen BR. Timpl R. Structure, function and tissue forms of the C-terminal globular domain of collagen XVIII containing the angiogenesis inhibitor endostatin. EMBO Journal 1998; 17(15):4249-56
7. Zetter BR. Angiogenesis and tumor metastasis. Annual Review of Medicine 1998; 49:407-24
8. Hohenester E. Sasaki T. Olsen BR. Timpl R.: Crystal structure of the angiogenesis inhibitor endostatin at 1.5 A resolution. EMBO Journal 1998; 17(6):1656-64
9. Horsman MR, et al: The effect of shark cartilage extracts on the growth and metastatic spread of the SCCVII carcinoma. Acta Oncol. 1998; 37(5): 441-5.
10. Miller DR, et al: Phase I/II trial of the safety and efficacy of shark cartilage in the treatment of advanced cancer. J Clin Oncol. 1998; 16(11):3649-55
11. Simone CB, et al: Shark cartilage for cancer. Lancet. 1998; 9; 351(9113): 1440.
12. Newman V, et al: Dietary supplement use by women at risk for breast cancer recurrence. The Women's Healthy Eating and Living Study Group. J Am Diet Assoc. 1998; 98(3): 285-92.
13. Ernst E: Shark cartilage for cancer? Lancet. 1998; 24; 351(9098): 298.
14. Markman M: Shark cartilage: the Laetrile of the 1990s. Cleve Clin J Med. 1996; 63(3): 179-80.
15. Hunt TJ, et al: Shark cartilage for cancer treatment. Am J Health Syst Pharm. 1995; 52(16): 1756, 1760.
16. Blackadar CB: Skeptics of oral administration of shark cartilage. J Natl Cancer Inst. 1993; 85(23): 1961-2.
17. Mathews J: Media feeds frenzy over shark cartilage as cancer treatment. J Natl Cancer Inst. 1993; 4; 85(15): 1190-1.
18. Oikawa T, et al: A novel angiogenic inhibitor derived from Japanese shark cartilage (I). Extraction and estimation of inhibitory activities toward tumor and embryonic angiogenesis.Cancer Lett. 1990;51(3):181-6.
19. Lee A, et al: Shark cartilage contains inhibitors of tumor angiogenesis. Science. 1983; 221 (4616):1185-7.
20. Langer R. Brem H. Falterman K. Klein M. Folkman J. Isolations of a cartilage factor that inhibits tumor neovascularization. Science; 1976. 193(4247):70-2
21. Couzin J.: Beefed-up NIH center probes unconventional therapies. Science. 1998 Dec 18; 282(5397):2175-6
22. Laurent ,T. C. (1987): Biochemistry of hyaluronan. Acta Otolaryngol; 442: 7-24
23. Schwatz, N. B. : Proteoglycans. In Devlin, T. M. ed (1992) Textbook of biochemistry with clinical correlations. A John wiley & Sons , Inc., New York 378-379
24. Laurent, T. C. (1970) Structure of hgyaluronic acid. In Balazs EA.ed. Chemistry and molecular biology of the intercellular matrix. London: Academic Press. 703-732

25. Roden, L. (1980) Structure and metabolism of connective tissue proteoglycans. In: Lennarz, W. J. ed. The biochemistry of glycoprotein and proteoglycans. New York: Plenum Publ. 267-371
26. Tengblad A.: Affinity chromatography on immobilized hyaluronate and its application to the isolation of hyaluronate binding properties from cartilage. Biochimica et Biophysica Acta. 578(2):281-9, 1979
27. Tengblad A: . A comparative study of the binding of cartilage link protein and the hyaluronate-binding region of the cartilage proteoglycan to hyaluronate-substituted Sepharose gel. B
28. Brooks PC, Silletti S, von Schalscha TL, Friedlander M, Cheresh DA: Disruption of angiogenesis by PEX, a noncatalytic metalloproteinase fragment with integrin binding activity. Cell 1998; 92(3):391-400

[CANCER RESEARCH 61, 1022–1028, February 1, 2001]

Metastatin: A Hyaluronan-binding Complex from Cartilage That Inhibits Tumor Growth[1]

Ningfei Liu,[2] Randall K. Lapcevich,[2] Charles B. Underhill, Zeqiu Han, Feng Gao, Glenn Swartz, Stacy M. Plum, Lurong Zhang,[2] and Shawn J. Green[2, 3]

Department of Oncology, Georgetown University Medical Center, Washington, D.C. 20007 [N. L., C. B. U., Z. H., F. G., L. Z.], and EntreMed, Inc., Rockville, Maryland 20902 [R. K. L., G. S., S. M. P., S. J. G.]

ABSTRACT

In this study, a hyaluronan-binding complex, which we termed Metastatin, was isolated from bovine cartilage by affinity chromatography and found to have both antitumorigenic and antiangiogenic properties. Metastatin was able to block the formation of tumor nodules in the lungs of mice inoculated with B16BL6 melanoma or Lewis lung carcinoma cells. Single i.v. administration of Metastatin into chicken embryos inhibited the growth of both B16BL6 mouse melanoma and TSU human prostate cancer cells growing on the chorioallantoic membrane. The *in vivo* biological effect may be attributed to the antiangiogenic activity because Metastatin is able to inhibit the migration and proliferation of cultured endothelial cells as well as vascular endothelial growth factor-induced angiogenesis on the chorioallantoic membrane. In each case, the effect could be blocked by either heat denaturing the Metastatin or premixing it with hyaluronan, suggesting that its activity critically depends on its ability to bind hyaluronan on the target cells. Collectively, these results suggest that Metastatin is an effective antitumor agent that exhibits antiangiogenic activity.

INTRODUCTION

A potential therapeutic target on angiogenic endothelial cells is hyaluronan, a large negatively charged glycosaminoglycan that plays a role in the formation of new blood vessels (1). Particularly high concentrations of hyaluronan are associated with endothelial cells at the growing tips or sprouts of newly forming capillaries (2, 3). Similarly, when cultured endothelial cells are stimulated to proliferate by cytokines, their synthesis of hyaluronan is significantly increased (4). Interestingly, this stimulation is restricted to endothelial cells derived from the small blood vessels and is not seen in endothelial cells derived from larger ones (4). In the case of mature blood vessels, hyaluronan is present in perivascular regions and in the junctions between the endothelial cells (5, 6). Earlier studies have shown that exogenously applied hyaluronan has different effects on angiogenesis depending on its size, with macromolecular hyaluronan inhibiting vascularization in chicken embryos, and oligosaccharide fragments of hyaluronan stimulating vascularization in the chorioallantoic membrane (7–9). Thus, hyaluronan appears to be specifically associated with the endothelial cells of newly forming blood vessels and can influence their behavior.

In addition to hyaluronan, endothelial cells involved in neovascularization also express CD44 and other cell surface receptors for hyaluronan (10–12). In particular, endothelial cells associated with tumors express large amounts of CD44 (11). In previous studies, we have shown that CD44 allows cells to bind hyaluronan so that it can be internalized into endosomal compartments, where the hyaluronan is degraded by the action of acid hydrolases (13, 14). Thus, the expression of CD44 by endothelial cells allows them to bind and internalize hyaluronan as well as any associated proteins. The fact that both hyaluronan and CD44 are up-regulated in endothelial cells involved in neovascularization suggests that the turnover of hyaluronan by these cells is much greater than that by cells lining mature blood vessels.

The increased turnover of hyaluronan in tumor-associated endothelial cells suggested a possible mechanism to specifically target these cells. Our initial idea was to use a hyaluronan-binding complex isolated from cartilage to deliver chemotherapeutic agents specifically to these endothelial cells. Purified by affinity chromatography, this hyaluronan-binding complex consists of tryptic fragments of the link protein and aggrecan core protein (5, 15, 16). We intended to couple the hyaluronan-binding complex to a chemotherapeutic agent such as methotrexate and use this derivative to attack endothelial cells. We hoped that this derivative would bind to the hyaluronan on the endothelial cells and then be internalized into lysosomes, where the methotrexate would be released by the action of acid hydrolyses. Surprisingly, however, in the course of these experiments, we found that the hyaluronan-binding complex by itself (*i.e.*, in the absence of a chemotherapeutic agent) inhibited angiogenic activity. Functionally, we termed the hyaluronan-binding complex, which inhibits tumor growth, Metastatin.

In the present study, we demonstrate that Metastatin has a number of intriguing biological activities, including inhibition of endothelial cell proliferation and migration, inhibition of angiogenesis, and suppression of tumor cell growth in chicken embryos and pulmonary metastasis in mice. These effects are blocked by preincubating Metastatin with hyaluronan, suggesting that the activity of Metastatin depends on its ability to bind hyaluronan on the target cells.

MATERIALS AND METHODS

Preparation of Metastatin. The hyaluronan-binding complex was prepared by a modified version of the method originally described by Tengblad (15, 16). Briefly, bovine nasal cartilage (Pel-Freez, Rogers, AR) was shredded with a Sure-Form blade (Stanley), extracted overnight with 4 M guanidine-HCl and 0.5 M sodium acetate (pH 5.8), and dialyzed against distilled water to which 10× PBS was added to a final concentration of 1× PBS (pH 7.4). The protein concentration was measured, and for each 375 mg of protein, 1 mg of trypsin (type III; Sigma, St. Louis, MO) was added. After digestion for 2 h at 37°C, the reaction was terminated by the addition of 2 mg of soybean trypsin inhibitor (Sigma) for each milligram of trypsin. The digest was dialyzed against 4 M guanidine-HCl and 0.5 M acetate (pH 5.8), mixed with hyaluronan coupled to Sepharose, and then dialyzed against a 10-fold volume of distilled water. The hyaluronan-Sepharose beads were placed into a chromatography column and washed with 1.0 M NaCl, followed by a gradient of 1.0–3.0 M NaCl. Metastatin was eluted from the hyaluronan affinity column with 4 M guanidine-HCl and 0.5 M sodium acetate (pH 5.8), dialyzed against saline, and sterilized by passage through a 0.2-μm-pore filter. For SDS-PAGE analysis, the purified preparation was loaded onto a 10% BisTris nonreducing gel (Novex, Inc.) and subsequently stained with Coomassie Blue. To identify the

Received 7/12/00; accepted 11/28/00.

The costs of publication of this article were defrayed in part by the payment of page charges. This article must therefore be hereby marked *advertisement* in accordance with 18 U.S.C. Section 1734 solely to indicate this fact.

[1] Supported in part by the United States Army Medical Research and Materiel Command under DAMD1717-94-J-4284, DAMD17-98-1-8099, and DAMD17-99-1-9031. Additional support was obtained from the Susan G. Komen Foundation and NIH Grant R29CA71545.

[2] These authors contributed equally to this work.

[3] To whom requests for reprints should be addressed, at EntreMed, Inc., Medical Center Drive, Suite 200, Rockville, MD 20902. Phone: (301) 738-2494; Fax (301) 217-9594; E-mail shawng@entremed.com.

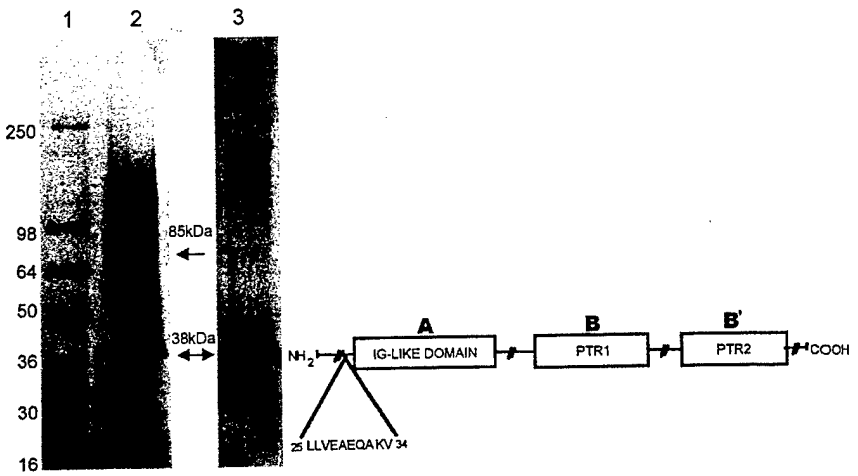

Fig. 1. SDS-PAGE and NH_2-terminal analysis of Metastatin. *Lane 1*, molecular mass markers; *Lane 2*, Metastatin stained with Coomassie blue; *Lane 3*, Western blot of Metastatin immunostained with an antibody against the link protein. The fragment of aggrecan migrated as a diffuse band at ~85 kDa, whereas the truncated link protein was at 38 kDa. NH_2-terminal sequence analysis of the 38-kDa band indicated that the first 24 amino acids of the link protein have been cleaved and is indicated on the schematic diagram.

link protein by Western blotting, the proteins on the gel were transferred to a sheet of nitrocellulose and immunostained with the 9/30/8-A-4 monoclonal antibody. (The monoclonal antibody, developed by Dr. B. Caterson, was obtained from the Developmental Studies Hybridoma Bank under the auspices of the NICHD and maintained by the University of Iowa, Department of Biological Sciences, Iowa City, IA 52242.) This identity was further confirmed by NH_2-terminal sequencing (Fig. 1). In tests of the biological activity of Metastatin, controls consisted of Metastatin mixed with an excess mass of hyaluronan (Lifecore, Chaska, MN) or a heat-inactivated preparation made by placing it in a boiling water bath for 30 min.

Endothelial and Tumor Cell Lines. HUVECs[4] were obtained from the Tumor Bank of the Lombardi Cancer Center (Georgetown University, Washington, DC). ABAEs were kindly provided by Dr. Luyuan Li (Lombardi Cancer Center), and BRECs were provided by Dr. Rosemary Higgins (Pediatrics, Georgetown University). These endothelial cells were cultured in 90% DMEM, 10% fetal bovine serum, and 10 ng/ml bFGF. The B16BL6 melanoma tumor line was obtained from the National Cancer Institute Central Repository (Frederick, MD), TSU cells were obtained from the American Type Culture Collection (Rockville, MD), and Lewis lung carcinoma cells were kindly supplied by Dr. Michael O'Reilly (Children's Hospital, Boston, MA). The tumor cells were grown in 90% DMEM, 10% fetal bovine serum, and 2 mM L-glutamine. For the mouse metastasis assays, cells were generally used between passages 6 and 18.

Mice. Specific pathogen-free, male, 6–8-week-old C57Bl/6 mice were obtained from The Jackson Laboratory (Bar Harbor, ME). Animals were cared for and treated in accordance with the procedures outlined in the Guide for the Care and Use of Laboratory Animals (NIH Publication No. 86-23). Animals were housed in a pathogen-free environment and provided with sterilized animal chow (Harlan Sprague Dawley, Indianapolis, IN) and water *ad libitum*.

Mouse Metastasis Model System. For the experimental melanoma model, mice were inoculated i.v. in the lateral tail vein with B16Bl6 cells (5×10^4 cells/animal) on day 0. Treatment was initiated on day 3 with 5 (0.2 mg/kg), 15 (0.6 mg/kg), and 49 μg (2 mg/kg) of Metastatin and continued daily until animals were sacrificed on day 14. After euthanasia, the lungs were removed, and surface metastatic lesions were enumerated under a dissecting microscope.

Mice were also inoculated with Lewis lung carcinoma cells, which aggressively form pulmonary metastases. Mice were injected i.v. in the lateral tail vein with 2.5×10^5 cells/animal (day 0), and beginning on day 3, the Metastatin was administered by daily i.p. injections of 15 (0.6 mg/kg) and 49 μg (2 mg/kg) or by three i.v. injections of 100 μg (4 mg/kg) on days 1, 3, and 5. Animals were euthanized, and their lungs were removed and weighed. To obtain the lung weight gain, the average lung weight of nontreated mice (0.2 g) was subtracted from that of the treated animals.

The number of pulmonary metastases and lung weight gains were reported as mean ± SD, and the differences were compared using Student's *t* test. The groups were considered to be different when the probability (*P*) value was <0.05.

Chicken Chorioallantoic Membrane Assays. To measure angiogenesis, a chick chorioallantoic membrane assay was performed using a modification of the methods of Brooks *et al.* (17). For this, holes were drilled in the tops of 10-day-old chicken eggs to expose the chorioallantoic membranes, and filter discs (0.5 cm in diameter) containing 20 ng of human recombinant VEGF [20 μl (1 μg/ml); Pepro, Rocky Hill, NJ] were placed on the surface of each chorioallantoic membrane (day 0). The holes were covered with parafilm, and the eggs were incubated at 37°C in a humidified atmosphere. One day later, the eggs were given injections (via a blood vessel in the chorioallantoic membrane using a 30-gauge needle) of the various substances [Metastatin (80 μg/egg) or controls consisting of PBS or heat-inactivated Metastatin]. Three days later (day 4), the chorioallantoic membranes and associated discs were cut out and immediately immersed in 3.7% formaldehyde. For computer-assisted image analysis, the discs were divided into quarters with fine wires, and the blood vessels in each quarter were digitally photographed and analyzed by an Optimas 5 program to calculate the vessel area and length normalized to the total area measured. The means and the SEs were calculated from all quadrants within each group, and the statistical significance was determined by Student's *t* test. Twelve or more eggs were used for each sample point.

For the growth of xenografts on the chorioallantoic membrane, holes were cut into the sides of 10-day-old eggs exposing the membrane (day 0), and then 1×10^6 B16BL6 or TSU cells were applied to the membranes. Two days later, the eggs were given i.v. injections of the various substances. On day 7, the tumor masses were fixed in formalin, dissected free from the normal membrane tissue, and weighed.

Cell Growth Assays. To determine the effects of Metastatin on cell growth, the cell lines were subcultured into 24-well dishes at a density of approximately 5×10^5 cells/well for the endothelial cell lines (HUVEC, ABAE, and BREC) and 5×10^4 cells/well for tumor cell lines (B16BL6, TSU, and Lewis lung carcinoma). For the dose-response experiments, the medium was changed every other day, and at the end of 6 days, the cells were released with 0.5 mM EDTA in PBS, and the cell number was determined with a Coulter counter (Hialeah, FL).

ELISA Assay for Hyaluronan. Cells were grown to confluence in 24-well dishes, and the conditioned medium was collected, incubated with a biotinylated version of the Metastatin (16), and then transferred to plates precoated with hyaluronan (umbilical cord; Sigma). The hyaluronan present in the conditioned medium interacts with the biotinylated Metastatin so that less of it will be left to bind to hyaluronan attached to the plate. At the end of the incubation, the plates were washed, and the amount of biotinylated Metastatin remaining attached was determined by incubating the plates with streptavidin coupled to peroxidase (Kirkegard & Perry, Gaithersburg, MD) followed by a soluble substrate for peroxidase. The amount of hyaluronan in the conditioned medium was calculated by comparison with a standard curve with known amounts of hyaluronan (16).

[4] The abbreviations used are: HUVEC, human umbilical vein endothelial cell; ABAE, adult bovine aorta endothelial cell; BREC, bovine retinal endothelial cell; VEGF, vascular endothelial growth factor; bFGF, basic fibroblast growth factor.

Wound Migration Assay. A suspension of HUVECs (5×10^5 cells in 5 ml of 98% M199 and 2% fetal bovine serum) was added to 60-mm tissue culture plates that had been precoated with gelatin (2 ml of 1.5% gelatin in PBS, 37°C, overnight) and allowed to grow for 3 days to confluence. An artificial "L"-shaped wound was generated in the confluent monolayer with a sterile razor blade by moving the blade down and across the plate. Plates were then washed with PBS, and 2 ml of PBS were added to each plate along with 2 ml of sample in M199 and 2% fetal bovine serum in the presence and absence of 5 ng/ml bFGF. After an overnight incubation, the plates were treated with Diff-Quik for 2 min to fix and stain the cells. The number of cells that migrated were counted under ×200 magnification using a 10-mm micrometer over a 1 cm distance along the wound edge. Ten fields for each plate were counted, and an average for the duplicate was calculated.

RESULTS

Characterization of Metastatin. Metastatin was isolated from bovine nasal cartilage by affinity chromatography on hyaluronan-Sepharose. As shown in Fig. 1, Metastatin consisted of two molecular factions as determined by SDS-PAGE, a sharp band at 38 kDa that corresponds to the link protein, and a diffuse band at approximately 85 kDa that represents a tryptic fragment of the aggrecan core protein (5, 15, 16). The diffuse nature of this latter fraction is probably due to variations in the degree of glycosylation and glycosaminoglycan content. The identity of the link protein was verified by immunoblotting with a specific monoclonal antibody against this protein (Fig. 1). In addition, NH_2-terminal sequence analysis of the 38-kDa band revealed that the purified protein was missing the first 24 amino acids. Previous studies have shown that this complex binds to hyaluronan with high affinity and specificity (5, 16). Indeed, a biotinylated version of the preparation has been widely used as a histochemical stain to localize hyaluronan in tissue sections (5, 16).

Because cartilage is known to contain various protease inhibitors, which may contribute to its antitumor properties (18), we wanted to determine whether Metastatin possessed such attributes. For this reason, we used a chromogenic assay (Diapharma Group, Inc., West Chester, OH) to assess the effect of Metastatin on the following enzymes: (*a*) trypsin; (*b*) chymotrypsin; (*c*) plasmin; and (*d*) elastase. At concentrations as high as 100 μg/ml, Metastatin did not inhibit the activity of any of the enzymes tested (data not shown).

Effect of Metastatin on Metastatic Tumors. In initial experiments, we found that Metastatin was effective at inhibiting pulmonary metastases of B16BL6 cells. When mice were given daily i.p. injections of Metastatin 3 days after tumor inoculation, lung metastases were strikingly reduced (Fig. 2*A*). Fig. 2*B* shows that the number of surface lung metastases (>0.5 mm) in the mice treated with 15 and 49 μg Metastatin/day were reduced by more than 80%. The dose-response curve shown in Fig. 2*C* was constructed from two independent experiments and shows that Metastatin decreased the number of metastatic colonies in a dose-dependent manner with an ED_{50} of approximately 10 μg (0.4 mg/kg). Significantly, when Metastatin preparations were premixed with macromolecular hyaluronan, the antimetastatic activity was blocked, and the mean number of surface pulmonary metastases was comparable to that seen in control mice (Fig. 2*B*). This suggests that the ability of Metastatin to bind hyaluronan is required for its anti-tumor activity.

Similar results were obtained with the Lewis Lung carcinoma cell line, which is a more aggressive mouse tumor model. As shown in Fig. 3, *A* and *B*, Metastatin inhibited pulmonary metastasis of Lewis lung carcinoma cells in a dose-related fashion, as reflected in the weight gain of the lungs. Furthermore, Metastatin was effective when given by two different routes, i.p. and i.v. (Fig. 3, *B* and *C*).

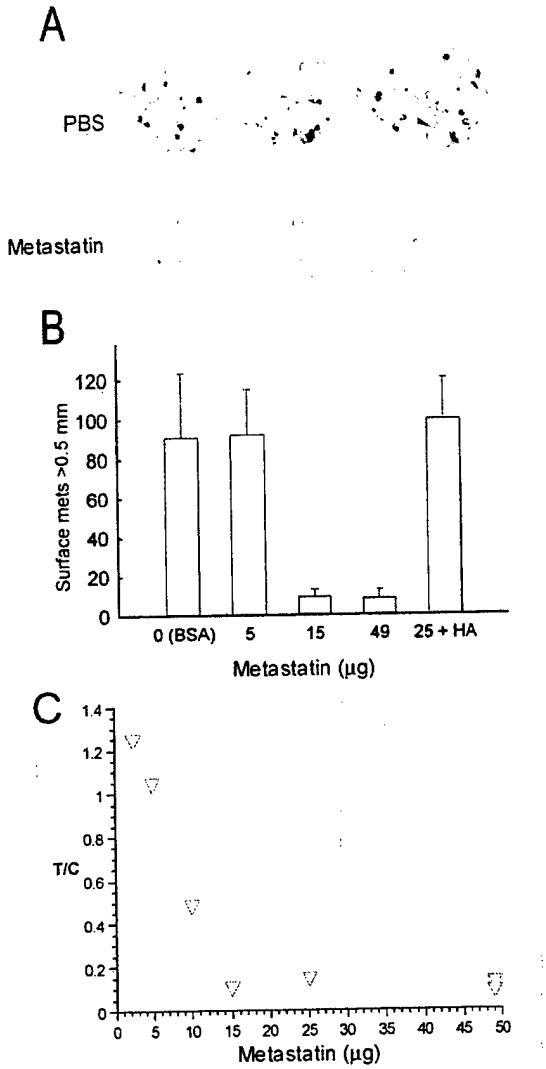

Fig. 2. Effect of Metastatin on B16BL6 melanoma metastasis. B16BL6 melanoma cells were injected into the tail veins of C57Bl/6 mice, and 3 days later, the mice were injected i.p. with increasing doses of Metastatin. After 14 days, the lungs were removed, and surface pulmonary metastases were counted. *A*, the lungs from control animals had a greater number of metastases than those from the Metastatin (49 μg)-treated animals. *B*, the number of pulmonary metastases larger than 0.5 mm is plotted against the concentration of Metastatin injected. Metastatin inhibits the number of metastases, and the addition of hyaluronan to Metastatin blocked its inhibitory activity. The values shown are the mean of at least five mice/group; *bars*, SD. *C*, this dose-response curve was derived from two independent experiments ($n = 5$ for each point) and shows the ratio of pulmonary metastasis in the test and control animals (*T/C*) as a function of the Metastatin dose.

Effect of Metastatin on *in Vitro* Cell Proliferation and Migration. In the next series of experiments, we wanted to determine whether Metastatin has any effect on the growth of either endothelial or tumor cells in tissue culture. For these experiments, the cells were grown in the presence of varying concentrations of Metastatin for 6 days, and then the final cell numbers were determined. Metastatin inhibited the proliferation of the endothelial cell lines HUVEC, ABAE, and BREC (Fig. 4*A*) and two of the tumor cell lines (B16BL6 and Lewis lung carcinoma cells) but had no effect on the TSU cells (Fig. 4*B*). Similar results were obtained when proliferation was monitored by incorporation of bromodeoxyuridine (data not shown). It is important to note that the growth inhibition of B16BL6 cells was partially blocked when the preparation of Metastatin was premixed with an excess of hyaluronan (Fig. 4*B*).

One possible explanation for the lack of TSU cell sensitivity to

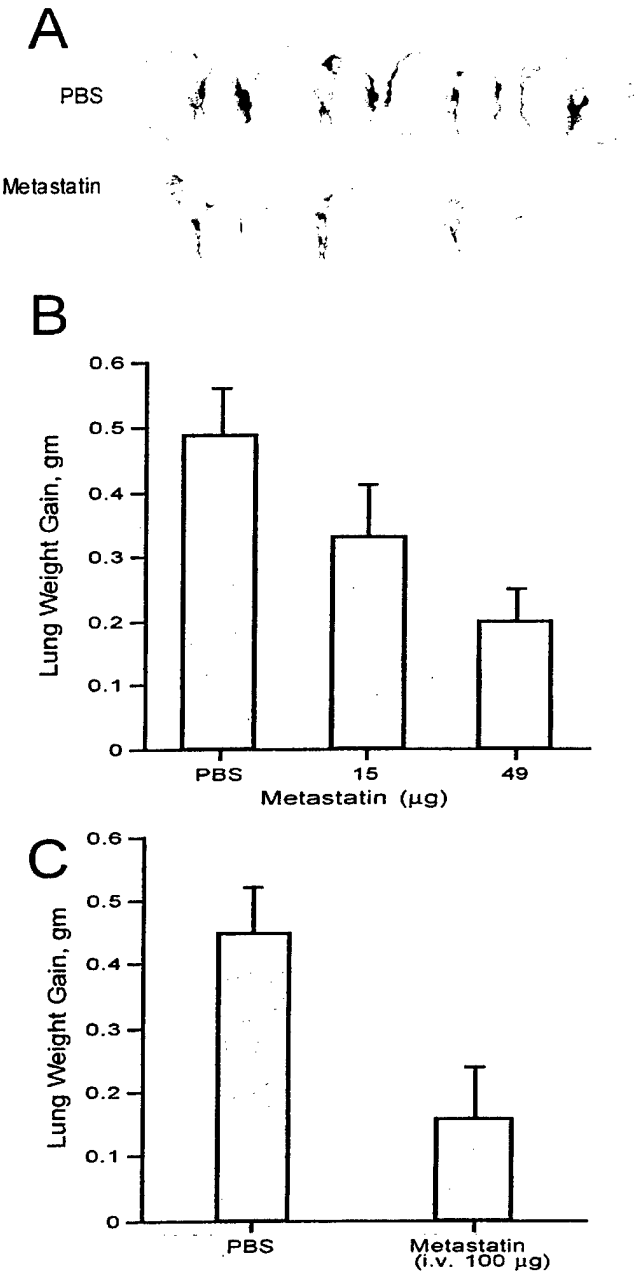

Fig. 3. Inhibition of pulmonary metastasis of Lewis lung carcinoma cells. Lewis lung carcinoma cells were injected into the tail veins of C57Bl/6 mice, and 3 days later, mice were treated with PBS or Metastatin. Once the treatment was stopped, animals were euthanized, and lungs were removed and weighed. *A*, shows representative lungs from control and treated animals and illustrates that Metastatin lowers the tumor burden. *B*, Metastatin injected i.p. daily beginning on day 4 decreased the relative lung weights in a dose-dependent fashion. *C*, the weight of the lungs in animals was also decreased when Metastatin was administered by three separate i.v. injections (100 μg/injection on days 1, 3, and 5). The values shown are the mean of at least five mice/group; *bars*, SD.

Metastatin could be the amount of hyaluronan that they secrete because it has an inhibitory effect. To test this possibility, conditioned media from confluent cultures of the different cell lines were collected and analyzed for hyaluronan by a modified ELISA. TSU cells were found to secrete significantly larger amounts of hyaluronan into the medium than the other cell lines (7 μg/ml *versus* <0.5 μg/ml, respectively). Indeed, this level of hyaluronan would be sufficient to block the effects of added Metastatin.

We also examined the effects of Metastatin on the migration of endothelial cells, another important factor in the process of angiogenesis (19). In this assay, we examined the effect of Metastatin on the migration of HUVECs using the wound migration assay. Fig. 5 shows that at a concentration of 10 μg/ml, Metastatin inhibited the migration of HUVECs by 50% as compared with controls treated with bFGF alone. Again, similar results were obtained when migration was monitored using Nucleopore filters (data not shown).

Effect of Metastatin on VEGF-induced Angiogenesis. The fact that Metastatin could inhibit both the growth and migration of endothelial cells *in vitro* suggested that it might also be able to block angiogenesis *in vivo*. To test this possibility, we examined the effect

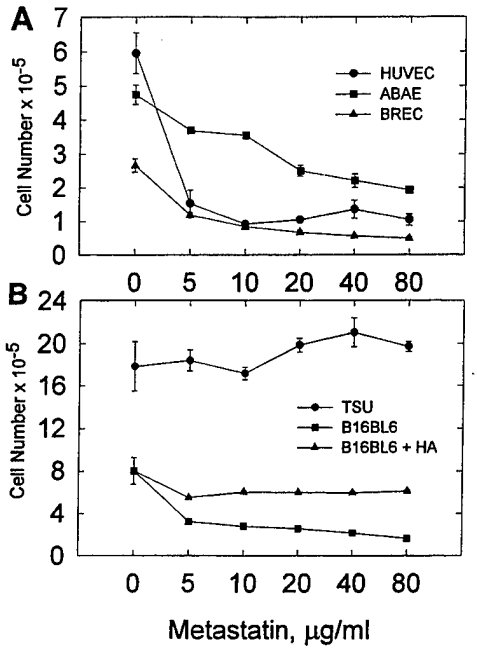

Fig. 4. The effects of varying concentrations of Metastatin on the growth of cultured cells. The cell lines were cultured in 24-well dishes in complete medium containing the indicated amounts of Metastatin, with medium changes ever other day. After 6 days, the cells were harvested with a solution of EDTA in PBS, and the cell numbers were determined with a Coulter counter. *A*, a dose-response curve is shown for the effects of Metastatin on the growth of the endothelial cell lines HUVEC, ABAE, and BREC. In each case, the growth of the cells was inhibited by Metastatin. *B*, a dose-response plot is shown for the tumor cell lines B16BL6 and TSU. Whereas Metastatin inhibited the growth of the B16BL6 cells, it had little or no effect on the TSU cells. The addition of an equal mass of hyaluronan to the Metastatin significantly reduced its effect on the proliferation of B16BL6 cells.

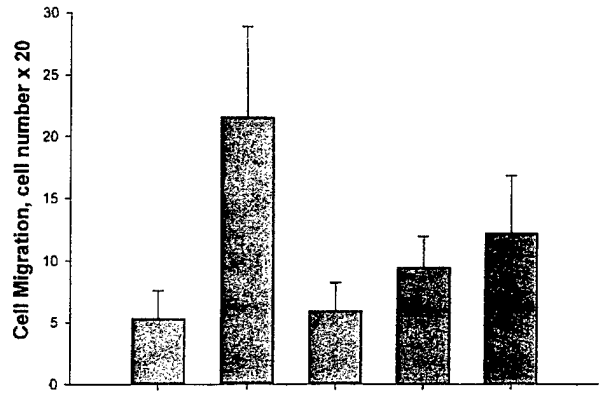

Fig. 5. Dose-dependent inhibitory effect of Metastatin on the migration of endothelial cells. HUVECs were grown to confluence on gelatin-coated culture plates, wounded with a sterile razor blade, and induced to migrate with bFGF in the presence of varying amounts of Metastatin. The number of cells that migrated were enumerated using a micrometer and microscope at ×200 magnification.

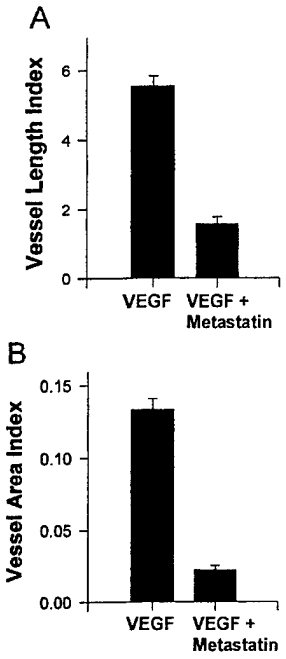

Fig. 6. Effect of Metastatin on VEGF-induced angiogenesis. The top of air sacs of 10-day-old chicken eggs were opened, exposing the chorioallantoic membranes, and filter discs containing 20 ng of VEGF were applied. The treated group was then injected i.v. with Metastatin (80 μg/egg), and the control group did not receive injections. The chorioallantoic membranes and associated discs were cut out on day 3 and analyzed by computer-assisted image analysis as described in "Materials and Methods". Metastatin had a significant inhibitory effect on both the (*A*) vessel length index and (*B*) vessel area index.

of Metastatin on angiogenesis induced in the chick chorioallantoic membrane. In this assay, filter papers containing recombinant human VEGF were placed on the chorioallantoic membrane of 10-day-old eggs, which were then given a single i.v. injection of the Metastatin or control preparations. Three days later, the extent of vascularization in the region of the filters was determined by computer-assisted image analysis. As shown in Fig. 6, treatment with Metastatin reduced both the length and area of vessels as compared with the control group, suggesting that Metastatin does indeed have the ability to block VEGF-induced angiogenesis.

Inhibition of Tumor Growth on the Chorioallantoic Membrane. To further explore the antitumor activity of Metastatin, we examined its effect on the growth of B16BL6 and TSU cells on the chicken chorioallantoic membrane. Tumor cells were applied to the chorioallantoic membranes of 10-day-old chicken embryos and allowed to grow for 1 week. Pilot experiments revealed that after inoculation with 10^6 cells, the take rate was almost 100% and resulted in xenografts with weights from 50–150 mg in 7 days. However, when the inoculated eggs were given a single i.v. injection of the Metastatin, the growth of the B16BL6 and TSU xenografts was greatly inhibited (Fig. 7). Again, this inhibitory effect was abolished if the preparation of Metastatin was heat inactivated or preincubated with its ligand, hyaluronan (Fig. 7*B*). It is important to note that Metastatin did not appear to adversely affect the development of the chicken embryos.

DISCUSSION

In this study we report that Metastatin, a cartilage-derived hyaluronan-binding complex consisting of proteolytic fragments of bovine link protein and aggrecan, is able to block the growth and metastasis of tumor cells under the following conditions: (*a*) a single i.v. injection of Metastatin into the chorioallantoic membrane of chicken embryos inhibited the growth of B16BL6 mouse melanoma cells and TSU human prostate cancer cells; (*b*) multiple i.p. injections of Metastatin prevented the experimental metastasis of B16BL6 and Lewis lung carcinoma cells to the lungs of mice; and (*c*) three i.v. injections of Metastatin were sufficient to inhibit the formation of Lewis lung carcinoma metastasis. In each case, Metastatin did not have an obvious detrimental effect on the host and was neutralized by complexing with soluble hyaluronan.

Metastatin is a member of a family of hyaluronan-binding proteins that also includes CD44, tumor necrosis factor-stimulated gene 6 (TSG-6), versican, neurocan, and brevican (20). Interestingly, Metastatin is similar to other factors that influence angiogenesis in that it is a fragment of a larger complex. For example, Angiostatin is a fragment of plasminogen, Endostatin represents a fragment of collagen XVIII, and serpin consists of a fragment of antithrombin (21–24). It is possible that the production of the peptide fragments is part of a feedback loop important in the down-regulation of angiogenesis.

In addition to Metastatin, a number of other antiangiogenic factors have been isolated from cartilage. Indeed, cartilage has been extensively studied as a source of molecules that could account for its avascular nature. Langer *et al.* (25) first reported a bovine cartilage fraction isolated by guanidine extraction and purified by trypsin affinity chromatography that inhibited tumor-induced vascular proliferation. In addition, Moses *et al.* (26) have recently isolated Troponin I from veal scapulae, which was shown to have antitumor and antiangiogenic properties. Lee and Langer (27) have described a guanidine-extracted factor from shark cartilage that inhibited angiogenesis and suppressed tumor vascularization. Similarly, Moses *et al.* (18) isolated a factor from cultures of scapular chondrocytes that inhibited angiogenesis in the chicken chorioallantoic membrane and appeared to be a protease inhibitor. However, it is likely that our preparation of Metastatin acts through a distinct mechanism because it has no detectable antiprotease activity and is inhibited by the addition of hyaluronan. It is tempting to speculate that Metastatin may contribute to the avascular nature of cartilage. Along these lines, we have previously found that hypertrophic chondrocytes produce large amounts of free hyaluronan, which may neutralize the effects of Metastatin in this region and thereby allow blood vessels to invade (28).

The results of this study suggest that Metastatin has antiangiogenic properties as demonstrated by its ability to block VEGF-induced formation of blood vessels in the chicken chorioallantoic membrane. The antiangiogenic effect of Metastatin was also consistent with our finding that it blocked both the proliferation and migration of cultured endothelial cells. Whereas Metastatin can directly attach tumor cells, we believe that most of its antitumor activity is due to its inhibition of angiogenesis because after its injection, the first cells that it would encounter are the endothelial cells, which would be exposed to the highest concentration. In addition, this antiangiogenic mechanism is suggested by the fact that Metastatin blocked the growth of TSU cells *in vivo* (*i.e.*, on the chicken chorioallantoic membrane) but had little or no effect on their proliferation *in vitro*. In this particular case, it seems likely that Metastatin was acting indirectly on the TSU tumor cells by blocking angiogenesis.

In other cases, the antitumor activity of Metastatin may be due to the combined action of direct killing of the tumor cells and the inhibition of angiogenesis. Indeed, Metastatin does appear to partially inhibit the growth of B16BL6 in tissue culture, and it could presumably have a similar effect *in vivo*. Because many blood vessels that are associated with tumors are leaky (29), Metastatin may be able to escape the circulation to interact directly with the tumor cells and block their proliferation. Along these lines, a recent study by Maniotis *et al.* (30) has indicated that some tumors have the ability to form

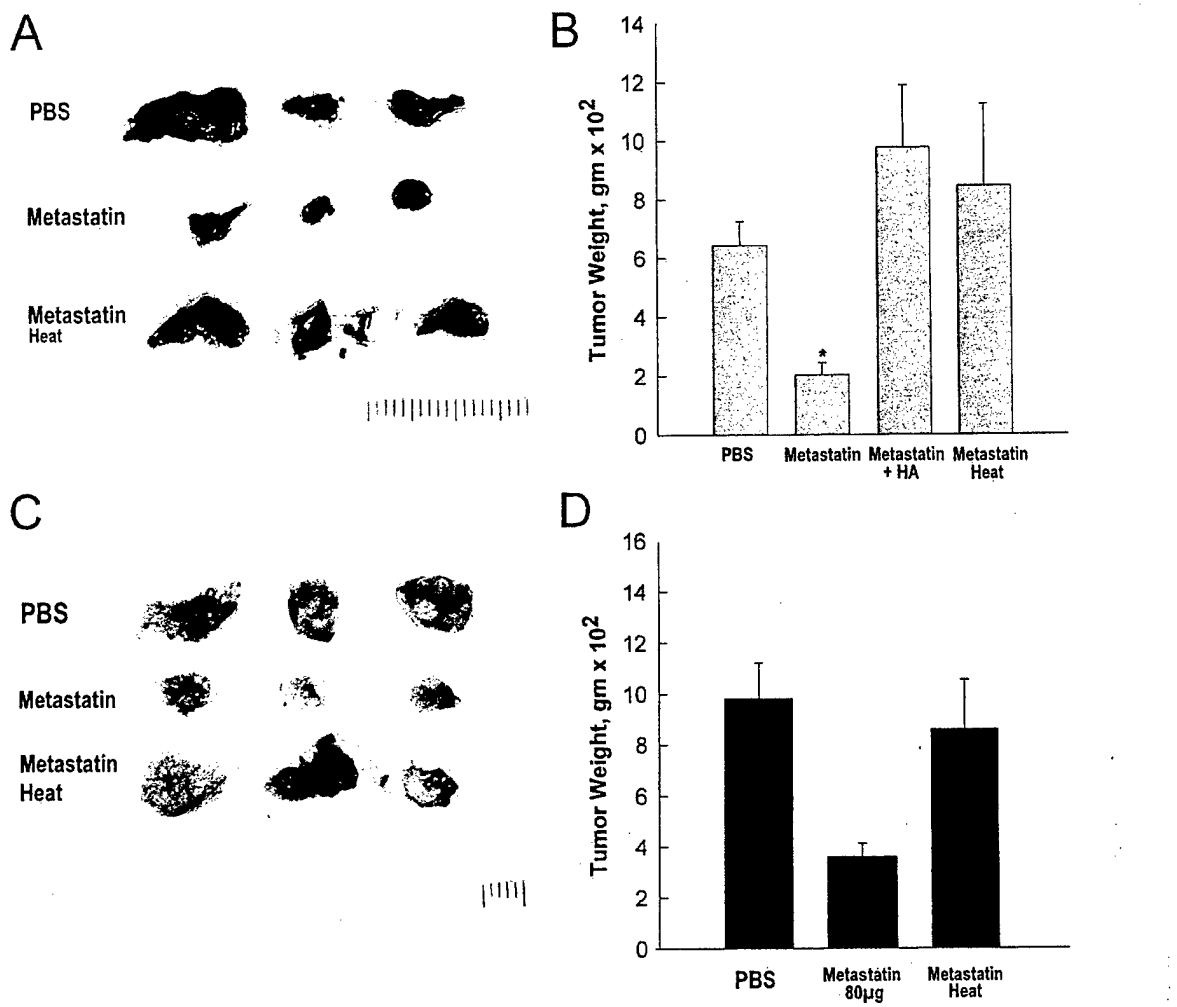

Fig. 7. Effect of Metastatin on the growth of tumor cells on the chicken chorioallantoic membrane. The top of the air sacs of 10-day-old chicken eggs were opened, exposing the chorioallantoic membrane, and pellets containing B16BL6 melanoma or TSU prostate tumor cells were placed on the membrane. On day 3, the embryos were given a single i.v. injection of PBS or Metastatin (80 μg). The tumors and associated chorioallantoic membranes were removed on day 6 and weighed. *A* and *C*, examples of the B16BL6 and TSU xenografts from eggs treated with PBS, Metastatin, or heat-denatured Metastatin. *B* and *D*, the weights of B16BL6 and TSU xenografts from eggs treated with Metastatin and control preparations are shown.

vasculature independent of endothelial cells. The tumor cells themselves appear to take on the characteristics of endothelial cells and are responsible for the formation of blood vessels. It is possible that such dual-acting tumor cells could also respond to Metastatin.

The biological effects of Metastatin appear to be closely linked to its ability to bind hyaluronan. If the preparation of Metastatin was premixed with hyaluronan, then this reversed its inhibitory effects on tumor growth *in vivo* and *in vitro* and its effects on the growth and migration of cultured endothelial cells. This indirectly suggests that Metastatin is binding to hyaluronan associated with the target cell. In the case of endothelial cells, particularly high levels of hyaluronan are localized to the tips of newly forming capillaries in the chicken chorioallantoic membrane and rabbit cornea (2, 3). A variety of other cell types show a similar relationship between proliferation and the production of hyaluronan (31–34). Whereas the hyaluronan present on proliferating tumor and endothelial cells could interact directly with Metastatin in the blood, the hyaluronan in other locations would not be exposed to high concentrations of the complex. Most normal cells would be protected by the fact that high concentrations of hyaluronan are present in connective tissues such as the dermis, lamina propria, and capsules (5, 35, 36), which would help to neutralize the Metastatin that diffused into these regions. It is important to note that under normal physiological conditions, hyaluronan in the blood is maintained at low levels by the liver and lymphatic system (37, 38). Thus, the circulating Metastatin should retain its hyaluronan binding activity.

Cell surface hyaluronan may serve as a target for other inhibitors of angiogenesis and tumor growth. For example, Endostatin, a ~20-kDa fragment of the COOH-terminal of collagen XVIII that inhibits angiogenesis (21, 22), may also be able to bind hyaluronan, as suggested by the presence of specific structural motifs (39). Secondly, a soluble, recombinant version of immunoglobulin fused with CD44 that binds to hyaluronan can inhibit the growth of human lymphoma cells that express CD44 in nude mice (40, 41). TSG-6, which is secreted by a variety of cells after stimulation with inflammatory cytokines, is able to both bind hyaluronan and block tumor cell growth (42). In each of these cases, these factors may be interacting with hyaluronan on the surfaces of target cells to exert their effects on angiogenesis and tumor growth.

In preliminary studies, we have found that Metastatin induces apoptosis in the target cells. However, at present, the mechanism by which Metastatin is able to do this is unclear. One possibility is that after Metastatin has bound to hyaluronan on the cell surface, it is taken up by the cells into lysosomes, where it is broken down into smaller fragments that enter the cytoplasm and induce apoptosis, perhaps by interacting with the mitochondrial membrane. Alternatively, Metasta-

tin could be interacting directly with the plasma membrane of the target cells, causing damage that in turn induces the apoptotic cascade. Clearly, future experiments will be directed toward elucidating the mechanism by which Metastatin induces apoptosis in the target cells.

In conclusion, we have found that Metastatin is able to block tumor growth in two model systems, and this effect depends on its ability to bind hyaluronan. Metastatin appears to target both tumor cells and endothelial cells that are involved in neovascularization. We postulate that during angiogenesis, the endothelial cells up-regulate their synthesis of hyaluronan, which then serves as a target for the injected Metastatin. Thus, Metastatin may represent a new type of antitumor agent, which targets cell surface hyaluronan.

ACKNOWLEDGMENTS

We are grateful to Dr. Theresa LaVallee and Wendy Hembrough for their assistance with the migration assay.

REFERENCES

1. Rooney, P., Kumar, S., Ponting, J., and Wang, M. The role of hyaluronan in tumor neovascularization. Int. J. Cancer, *60:* 632–636, 1995.
2. Ausprunk, D. H., Boudreau, C. L., and Nelson, D. A. Proteoglycans in the microvasculature. II. Histochemical localization in proliferating capillaries of the rabbit cornea. Am. J. Pathol., *103:* 367–375, 1981.
3. Ausprunk, D. H. Distribution of hyaluronic acid and sulfated glycosaminoglycans during blood vessel development in the chick chorioallantoic membrane. Am. J. Pathol., *177:* 313–331, 1986.
4. Mohamadzadeh, M., DeGrendele, H., Arizpe, H., Estess, P., and Siegelman, M. Proinflammatory stimuli regulate endothelial hyaluronan expression and CD44/HA-dependent primary adhesion. J. Clin. Investig., *101:* 97–108, 1998.
5. Green, S. J., Tarone, G., and Underhill, C. B. The distribution of hyaluronate and hyaluronate receptors in the adult lungs. J. Cell Sci., *89:* 145–156, 1988.
6. Eggli, P. S., and Graber, W. Association of hyaluronan with rat vascular endothelial and smooth muscle cells. J. Histochem. Cytochem., *43:* 689–697, 1995.
7. Feinberg, R. N., and Beebe, D. C. Hyaluronate in vasculogenesis. Science (Washington DC), *220:* 1177–1179, 1983.
8. West, D. C., Hampson, I. N., and Kumar, S. S. Angiogenesis induced by degradation products of hyaluronic acid. Science (Washington DC), *228:* 1324–1326, 1985.
9. Deed, R. P., Rooney, P. L., Kumar, J. D., Norton, J., Smith, A., Freemont, J., and Kumar, S. Early-response gene signaling is induced by angiogenic oligosaccharides of hyaluronan in endothelial cells. Inhibition by non-angiogenic, high-molecular-weight hyaluronan. Int. J. Cancer, *71:* 251–256, 1997.
10. Banerjee, S. D., and Toole, B. P. Hyaluronan-binding protein in endothelial cell morphogenesis. J. Cell Biol., *119:* 643–652, 1992.
11. Griffioen, A. W., Goenen, M. J. H., Damen, C. A., Hellwig, S. M. M., van Weering, D. H. J., Vooys, W., Blijham, G. H., and Groenewegen, G. CD44 is involved in tumor angiogenesis; an activation antigen on human endothelial cells. Blood, *90:* 1150–1159, 1997.
12. Banerji, S., Ni, J. Wang, S-X., Clasper, S., Su, J., Tammi, R., Jones, M., and Jackson, D. G. LYVE-1, a new homologue of the CD44 glycoprotein, is a lymph-specific receptor for hyaluronan. J. Cell Biol., *144:* 789–801, 1999.
13. Culty, M., Nguyen, H. A., and Underhill, C. B. The hyaluronan receptor (CD44) participates in the uptake and degradation of hyaluronan. J. Cell Biol., *116:* 1055–1062, 1992.
14. Culty, M., Shizari, M., Thompson, E. W., and Underhill, C. B. Binding and degradation of hyaluronan by human breast cancer cell lines expressing different forms of CD44: correlation with invasive potential. J. Cell. Physiol., *160:* 275–286, 1994.
15. Tengblad, A. Affinity chromatography on immobilized hyaluronate and its applications to the isolation of hyaluronate binding proteins from cartilage. Biochim. Biophys. Acta., *578:* 281–289, 1979.
16. Underhill, C. B., and Zhang, L. Analysis of hyaluronan using biotinylated hyaluronan-binding proteins. Methods Mol. Biol., *137:* 441–447, 1999.
17. Brooks, P. C., Silletti, S., von Schalscha, T. L., Friedlander, M., and Cheresh, D. A. Disruption of angiogenesis by PEX, a noncatalytic metalloproteinase fragment with integrin binding activity. Cell, *92:* 391–400, 1998.
18. Moses, M. A., Sudhalter, J., and Langer, R. Isolation and characterization of an inhibitor of neovascularization from scapular chondrocytes. J. Cell Biol., *119:* 473–482, 1992.
19. Ausprunk, D. H., and Folkman, J. Migration and proliferation of endothelial cells in preformed and newly formed blood vessels during tumor angiogenesis. Microvasc. Res., *14:* 53–65, 1977.
20. Neame, P. J., and Barry, F. P. The link protein. Experientia (Basel), *49:* 393–402, 1993.
21. Folkman, J., and Shing, Y. Angiogenesis. J. Biol. Chem., *267:* 10931–10934, 1992.
22. O'Reilly, M. S., Boehm, T., Shing, Y., Fukai, N., Vasios, G., Lane, W. S., Flynn, E., Birkhead, J. R., Olsen, B. R., and Folkman, J. Endostatin. An endogenous inhibitor of angiogenesis and tumor growth. Cell, *88:* 277–285, 1997.
23. O'Reilly, M. S., Holmgren, L., Shing, Y., Chen, C., Rosenthal, R. A., Moses, M., Lane, W. S., Cao, Y., Sage, E. H., and Folkman, J. Angiostatin. A novel angiogenesis inhibitor that mediates the suppression of metastases by a Lewis lung carcinoma. Cell, *79:* 315–328, 1994.
24. O'Reilly, M. S., Pirie-Sheperd, S., Lane, W. S., and Folkman, J. Antiangiogenic activity of the cleaved conformation of the serpin antithrombin. Science (Washington DC), *285:* 1926–1928, 1999.
25. Langer, R., Brem, H., Falterman, K., Klein, M., and Folkman, J. Isolations of a cartilage factor that inhibits tumor neovascularization. Science (Washington DC), *193:* 70–72, 1976.
26. Moses, M. A., Wiederschain, D., Wu, I., Fernandez, C. A., Ghazizadeh, V., Lane, W. S., Flynn, E., Sytkowski, A., Tao, T., and Langer, R. Troponin I is present in human cartilage and inhibits angiogenesis. Proc. Natl. Acad. Sci. USA, *96:* 2645–2650, 1999.
27. Lee, A., and Langer, R. L. Shark cartilage contains inhibitors of tumor angiogenesis. Science (Washington DC), *221:* 1185–1187, 1983.
28. Pavasant, P., Shizari, M., and Underhill, C. B. Distribution of hyaluronan in the epiphysial growth plate: Turnover by CD44 expressing osteoprogenitor cells. J. Cell Sci., *107:* 2669–2677, 1994.
29. Dvorak, H. F., Nagy, J. A., Dvorak, J. T., and Dvorak, A. M. Identification and characterization of the blood vessels of solid tumors that are leaky to circulating macromolecules. Am. J. Pathol., *133:* 95–109, 1988.
30. Maniotis, A. J., Folberg, R., Hess, A., Seftor, E. A., Gardner, L. M. G., Pe'er, J., Trent, J. M., Meltzer, P. S., and Hendirx, M. J. Vascular channel formation by human melanoma cells *in vivo* and *in vitro*: vasculogenic mimicry. Am. J. Pathol., *155:* 739–752, 1999.
31. Main, N. Analysis of cell-growth-phase-related variation in hyaluronate synthase activity of isolated plasma-membrane fractions of cultured human skin fibroblasts. Biochem. J., *237:* 333–342, 1986.
32. Tomida, M., Koyama, H., and Ono, T. Induction of hyaluronic acid synthetase activity in rat fibroblasts by medium change of confluent cultures. J. Cell. Physiol., *86:* 121–130, 1975.
33. Hronowski, L., and Anastassiades, T. P. The effect of cell density on net rates of glycosaminoglycan synthesis and secretion by cultured rat fibroblasts. J. Biol. Chem., *255:* 10091–10099, 1980.
34. Matuoka, K., Namba, M., and Mitsui, Y. Hyaluronate synthetase inhibition by normal and transformed human fibroblasts during growth reduction. J. Cell Biol., *104:* 1105–1115, 1987.
35. Alho, A. M., and Underhill, C. B. The hyaluronate receptor is preferentially expressed on proliferating epithelial cells. J. Cell Biol., *108:* 1557–1565, 1989.
36. Underhill, C. B. The interaction of hyaluronate with the cell surface: the hyaluronate receptor and the core protein. CIBA Found. Symp., *143:* 87–106, 1989.
37. Fraser, J. R. E., Appelgren, L. E., and Laurent, T. C. Tissue uptake of circulating hyaluronic acid. Cell Tissue Res., *233:* 285–293, 1983.
38. Laurent, T. C., and Fraser, J. R. E. The properties and turnover of hyaluronan. Laurent, removal of HA from the blood. CIBA Found. Symp., *124:* 9–29, 1986.
39. Hobenester, E., Sasaki, T., Olsen, B. R., and Timpl, R. Crystal structure of the angiogenesis inhibitor endostatin at 1.5 A resolution. EMBO J., *17:* 1656–1664, 1998.
40. Sy, M-S., Guo, Y. J., and Stamenkovic, I. Inhibition of tumor growth *in vivo* with a soluble CD44-immunoglobulin fusion protein. J. Exp. Med., *176:* 623–627, 1992.
41. Yu, Q., Toole, B. P., and Stamenkov, I. Induction of apoptosis of metastatic mammary carcinoma cells *in vivo* by disruption of tumor cell surface CD44 function. J. Exp. Med., *186:* 1985–1996, 1997.
42. Wisniewski, H. G., Hua, J-C., Poppers, D. M., Naime, D., Vilcek, J., and Cronstein, B. N. TSG-6, a glycoprotein associated with arthritis, and its ligand hyaluronan exert opposite effects in a murine model of inflammation. J. Immunol., *156:* 1609–1615, 1996.

40

Analysis of Hyaluronan Using Biotinylated Hyaluronan-Binding Proteins

Charles B. Underhill and Lurong Zhang

1. Introduction

In this chapter, we describe the preparation and use of b-PG, a biotinylated complex that specifically binds hyaluronan *(1,2)*. The b-PG is derived from cartilage and consists of a trypsin fragment of the proteoglycan core protein and one of the link proteins. Because of its ability to bind to hyaluronan with high affinity and specificity, the b-PG agent has proved to be useful in the histochemical localization of hyaluronan and its quantitative analysis by an enzyme linked assay *(1,2)*.

The b-PG reagent described here has evolved from several earlier versions. The first use of fluorescently tagged cartilage proteins for histochemistry of hyaluronan was described by Knudson and Toole *(3)*. Shortly after, Ripellino et al. described the use of a biotinylated reagent that was isolated from cartilage by ultracentrifugation *(4)*. The present protocol consists of a modification of one originally described by the late Dr. A. Tengblad that involves the use of affinity chromatography *(5)*. It should be acknowledged that the procedure describe here draws heavily from the excellent work of Dr. Tengblad.

While b-PG is a very useful reagent, its preparation is a major undertaking. The synthesis of HA-Sepharose and the purification of b-PG is both expensive and time consuming. Once the HA-Sepharose has been prepared, the isolation of b-PG takes about 2 wk. In general, we prepare several batches of the b-PG at one time, until we have exhausted our supply of cartilage extract. On the positive side, the HA-Sepharose can be reused many times, and the preparations of b-PG can be stored under the appropriate conditions for a number of years without loss of activity.

In the following sections we will describe:

1. The preparation of HA-Sepharose;
2. The isolation of b-PG;
3. The use of b-PG in histochemistry; and
4. The quantitative analysis of hyaluronan using b-PG in an enzyme linked assay.

From: *Methods in Molecular Biology, Vol. 137: Developmental Biology Protocols, Vol. III*
Edited by: R. S. Tuan and C. W. Lo © Humana Press Inc., Totowa, NJ

2. Materials

2.1. Preparation of HA-Sepharose

1. The NH_2-derivatized matrix, EAH Sepharose 4B is purchased from Pharmacia Biotech (Uppsala, Sweden). In general, we use 100 mL (two batches) of the matrix for each preparation. Alternatively, the derivatized matrix can be prepared according to the methods described by Cambiaso et al. *(6)*.
2. Highly purified hyaluronan of approx 7×10^5 molecular weight is obtained from Lifecore Biomedical (Chaska, MN).
3. Testicular hyaluronidase (type VI-S), 1-ethyl-3-(3-dimethylamino-propyl)carbodiimide and the other incidental reagents are obtained from Sigma Chemical Co. (St. Louis, MO).

2.2. Isolation of b-PG

1. Bovine nasal cartilage is purchased from Pel-Freez (Rogers, AR).
2. For processing of the cartilage, we use a Surform pocket plane (Stanley Tools) that is available in most hardware stores and cheese cloth that can be obtained at most grocery stores. In addition, large size dialysis tubing (3.3-cm Spectrapor membrane tubing) was used. In place of a Surform plane, a meat grinder may also be used.
3. Trypsin (type III) and soybean trypsin inhibitor (Type I-S) are both obtained from Sigma.
4. The biotinylating reagent Sulfo-NHS-LC-Biotin (EZ-Link) is obtained from Pierce (Rockford, IL).
5. Because the procedure requires large amounts of 4 *M* guanidine HCl, 0.5 *M* Na acetate pH 5.8, it is worthwhile to purify crude preparations of this reagent. To do this, 1528 g of practical grade guanidine HCl (Sigma) and 272 g of Na acetate-3 H_2O is dissolved in water, the pH is adjusted to 5.8 and the volume to 4 L. A tablespoon full of decolorizing carbon (Norit, Baker, NJ) is added to the solution which is stirred for 1 h. The solution is then passed through a Whatman filter on Buchner funnel and stored for use.

2.3. Histochemistry for Hyaluronan

1. The normal histochemical reagents consist of a clearing agent (Americlear), ethyl alcohol, and 30% H_2O_2.
2. A 10X stock solution of calcium–magnesium-free phosphate-buffered saline (PBS-A) is prepared from the following: 80 g NaCl, 2.0 g KH_2PO_4, 2.0 g KCl, and 11.5 g Na_2HPO_4 dissolved in 1 L of water. After diluting 1 to 10, the pH should be 7.3.
3. The reagent buffer consists of 90% PBS-A, 10% calf serum which should be passed through a 0.45 μm filter prior to use. This may be frozen in 10-mL aliquots.
4. Streptavidin-horse radish peroxidase can be purchased from Kirkegaard and Perry (Gaithersburg, MD).
5. The 3-amino-9-ethylcarbazole, dimethyl formamide (or dimethyl sulfoxide) and Mayer's hematoxylin solution are purchased from Sigma.
6. Crystal/mount to preserve the chromogens is purchased from Biomedia (Foster City, CA).

2.4. Enzyme Linked Assay for Hyaluronan

1. Hyaluronan was purchased from Lifecore Biomedical.
2. Bovine serum albumin, 2,2'azinobis (3-ethylbenzthiazoline sulfonic acid), 1-ethyl-3-(3-dimethylamino-propyl)carbodiimide and NaN_3 are purchased from Sigma.

3. Methods

3.1. Preparation of HA-Sepharose

The b-PG is isolated by affinity chromatography on a matrix of hyaluronan coupled to Sepharose (HA-Sepharose). The preparation of the HA-Sepharose involves two steps. In the first step, hyaluronan is converted to an appropriate size so it can penetrate the gel, and in the second step it is coupled to an NH_2-derivatized gel using a carbodiimide cross-linking agent. While the preparation of this gel is expensive, it can be reused many times.

1. To convert hyaluronan to the appropriate size, 1 g of the hyaluronan is dissolved in 500 mL of 0.15 *M* NaCl, 0.15 *M* Na acetate pH 5.0 and then incubated with 4000 U of testicular hyaluronidase (type VI-S, Sigma) for 3 h at room temperature. The digestion is stopped by placing the sample in a boiling water bath for 20 min and then the sample is centrifuged (10,000*g*, 15 min) to remove any precipitate. Four volumes of ethyl alcohol are added to the solution, which is cooled to –20°C for 1 h and then centrifuged (10,000*g*, 15 min) and the pellet of digested hyaluronan is collected. The precipitate is washed once in 75% alcohol to remove the acetate buffer.
2. For the coupling reaction, the digested hyaluronan (approx 1 g) is redissolved in a small volume of distilled water, mixed with 100 mL of the EAH Sepharose 4B and brought to a final volume of 250 mL. The suspension is placed on a shaking table (to avoid shearing the beads with a magnetic stirrer), the pH is adjusted to 4.7 and 2 g of the coupling agent 1-ethyl-3-(3-dimethylamino-propyl) carbodiimide is added to the mixture. Thereafter, the pH is continuously adjusted to 4.7 until the reaction has been completed (approx 3 h).
3. The mixture is allowed to sit over night, and then 10 mL of acetic acid is added to the suspension for a period of 6 h to block residual coupling agent. The gel is then transferred to a Buchner funnel and washed sequentially with 1 L each of: (a) 1 *M* NaCl, (b) 0.05 *M* formic acid, and (c) distilled water. The preparation is finally washed with 0.5 *M* Na acetate pH 5.7 plus a small amount of Na azide and is stored in this buffer at 4°C (*see* **Note 1**). The gel is stable for years.

3.2. Isolation of b-PG

The preparation of b-PG involves a number of steps. First, the extract is treated with trypsin to reduce its size. Second, the biotin-coupling reaction is carried out on the crude preparation so that endogenous hyaluronan protects the binding site. And finally, affinity chromatography is carried out taking advantage of the fact that the binding of aggrecan to hyaluronan is reversed by 4 *M* guanidine HCl.

1. The bovine nasal cartilage is thawed out and stripped of associated membranes with a pair of pliers, and then shredded with a Surform pocket plane. This step may take 1 d.
2. The shredded cartilage is weighed and mixed with 10 mL of 4 *M* guanidine HCl, 0.5 *M* Na acetate pH 5.8 for each gram of cartilage. The mixture is placed in a large beaker and placed on a shaking table at 4°C overnight (the solution is generally too thick to use a stirring bar).
3. To remove the solid material, pour the extract through several layers of prewashed cheese cloth. The fluid is then centrifuged (10,000*g*, 45 min, 4°C) and the supernatant is passed through a filter paper (Whatman no. 1, Whatman, Clifton, NJ) on a Buchner funnel.
4. The extract is then placed in large dialysis tubes (3.3 cm) and dialyzed against running tap water (leave plenty of room for the swelling of the dialysis bag because of osmosis).

Dialyze first against running tap water overnight and then against several changes of distilled water (it is necessary to remove the last traces of guanidine HCl that interfere with the biotin reaction).

5. The dialyzed extract is then lyophilized for long-term storage. For this, the extract is poured into ice cube trays, frozen, and then placed in a lyophilization bottle. This step may take several days (*see* **Note 2**).
6. Approximately 3 g of the lyophilized extract is mixed with 100 mL of 0.1 *M* HEPES, 0.1 *M* Na acetate pH 7.3, and is stirred overnight at 4°C to dissolve. The resulting mixture will be opaque and lumpy. In some cases, it may be desirable to further dialyze this sample against the above buffer to make sure that all of the guanidine has been removed.
7. Add 1.6 mg of purified trypsin to the mixture and then incubate at 37°C with occasional stirring. As the digestion progresses, the extract becomes less viscous. After 2 h, the digestion is stopped by adding 2 mg of soybean trypsin inhibitor and the pH is adjusted to 8.0.
8. Assay the protein content of the extract using a coomassie blue staining reagent (it should be between 5–10 mg/mL). Using the total amount of protein as a basis, add 1/10 the weight of sulfo-NHS-LC biotin to the sample. Allow the coupling reaction to proceed for 1–2 h at room temperature.
9. Dialyze the extract against three changes of 500 mL each of 4 *M* guanidine HCl, 0.5 *M* Na acetate, pH 5.8. The guanidine solutions can be reused several times for the first two changes, however, the final concentration of the extract should be close to 4 *M* guanidine HCl, 0.5 *M* Na acetate, pH 5.8.
10. Using a Buchner funnel, wash 100 mL of the HA-Sepharose with 4 *M* guanidine HCl, 0.5 *M* Na acetate, pH 5.8. and then transfer this gel to a beaker containing the extract. The mixture is poured into a large dialysis bag (leaving room for expansion) and placed in a beaker with nine volumes of distilled water. For the first 4 h, it is important to resuspend the beads that have settled out by inverting the bag upside down every 30 min. The beaker is then shaken overnight on a rotary table in the cold room.
11. Degas the mixture in a vacuum and pour into a column of the appropriate size. The gel is then washed with 200 mL of 1 *M* NaCl followed by a 400-mL linear gradient of from 1 to 3 *M* NaCl. At this point, the column is connected to a fraction collector (2.5 mL fractions) and the specifically bound proteins are eluted with 4 *M* guanidine HCl, 0.5 *M* Na acetate, pH 5.8. Each fraction is monitored for protein and those containing most of the protein are pooled and dialyzed against 0.15 *M* NaCl (*see* **Note 3**).
12. The concentration is adjusted to 200 µg/mL and then mixed with an equal volume of glycerol (100 µg/mL final concentration). Between 1 and 3 mg of the b-PG is generally obtained. This can be stored at –20°C, and is stable for a number of years (*see* **Note 4**).

3.3. Histochemistry of Hyaluronan with b-PG

The b-PG reagent is excellent for the histochemical localization of hyaluronan in tissue sections.

1. While fixation in formaldehyde by itself results in adequate preservation, Lin et al. has found that acid formalin in 70% alcohol provides superior retention of hyaluronan *(7)*. The use of cetylpyridinium chloride to help retain the hyaluronan is not advised.
2. The fixed tissue can then be processed and sectioned by a variety of techniques. These include direct cryostat sectioning, as well as paraffin and polyester wax embedding *(8)*. Because hyaluronan has a very stable structure, preservation of its structural integrity is generally not a problem.

3. The sections are rehydrated, by two 5 min incubations in the following solutions. Clearing agent (Americlear); 100% ethyl alcohol; 95% alcohol, 75% alcohol, and then water. The sections are then incubated for 5 min in 10% H_2O_2 to inactivate endogenous peroxidases. The sections are then rinsed in two washes of water and finally in PBS-A.
4. The slides are placed on a moist sponge in a covered baking pan and overlaid with a solution of 8–10 μg/mL of b-PG dissolved in 10% calf serum, 90% PBS-A (make sure the sections do not dry out). After 1 h the slides are washed for 5 min in PBS-A.
5. The sections are incubated for 15 min with a 1–500 dilution of streptavidin coupled to horse radish peroxidase in 10% calf serum, 90% PBS-A. Following the incubation, the slides are washed for 5 min in PBS-A.
6. The sections are then incubated with a substrate for horse radish peroxidase. We use 3-amino-9-ethylcarbazole that is particularly sensitive and gives rise to an intense red precipitate *(9)*. This should be prepared immediately before use in the following manner:
   a. Dissolve 2 mg of 3-amino-9-ethylcarbazole in 0.5 mL of dimethyl formamide (or dimethyl sulfoxide).
   b. Mix with 9.5 mL of 0.05 *M* Na acetate, pH 5.0.
   c. Pass solution through a 0.45-μm filter. The solution should be clear at this point.
   d. Add 10 μL of 30% H_2O_2 (1 μL per mL).
   e. Apply substrate to the slides. The reaction product has an intense red color. The incubation time can vary from less than 5 min to more than 30 min depending upon the section. Monitor the progress of the reaction by observing the slide under low magnification.
   f. Stop the reaction by washing section in PBS-A (or distilled water for hematoxylin staining).
7. If counter staining is desired, then the section can be dipped in Mayer's hematoxylin for 4 min, and then washed sequentially in distilled water, PBS-A and finally distilled water.
8. For permanent preservation of the stain, the sections can be coated with Crystal/mount (Biomedia) before attaching a cover slip.
9. To control for nonspecific staining, two different procedure may be used. First, the b-PG may be mixed with 0.1 mg/mL hyaluronan prior to application to the section. Alternatively, the sections may be pretreated with hyaluronidase. In our hands, the nonspecific staining is minimal (*see* **Note 5**).

3.4. An Enzyme-Linked Assay for Hyaluronan

This assay is based upon the ability of a sample of hyaluronan to bind to b-PG in solution and prevent it from binding to hyaluronan that is attached to a plastic substrate *(2)*. In our hands, the assay is sensitive to concentrations of hyaluronan between 50 ng/mL and 1 μg/mL.

1. The first step of this protocol is to coat plates with hyaluronan. It is important to note that pure hyaluronan by itself does not attach to plastic surfaces or nitrocellulose (however, crude preparations of hyaluronan, which are often associated with protein, will stick via the protein). Our approach is to couple hyaluronan to bovine serum albumin (HA-BSA) that adheres tightly to the plastic. For this, 100 mg of hyaluronan is dissolved in 500 mL of 0.2 *M* NaCl and the pH is adjusted to 4.7. To this is added 100 mg of bovine serum albumin followed by 20 mg of 1-ethyl-3(3-dimethylaminopropyl) carbodiimide. The pH is maintained at 4.7 for 1 h and then the solution is dialyzed extensively against PBS-A. The HA-BSA is aliquoted into 96 well plates (100 μL/well) and incubated for 30 min. The wells of the plate are then washed with PBS-A and then blocked with 10% calf serum, 90% CMF-PBS.

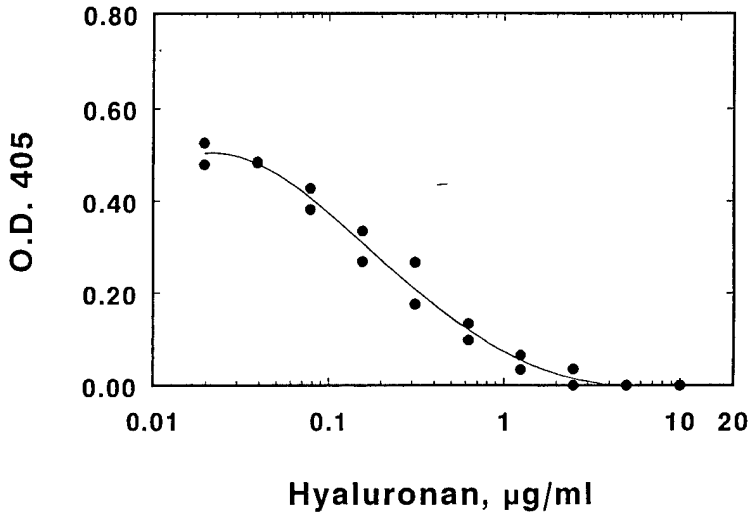

Fig. 1. Example of a standard curve for hyaluronan using the b-PG enzyme-linked assay. Varying amounts of standard hyaluronan were mixed with a set amount of b-PG and the mixtures were added to wells of a microtiter plate that had been precoated with HA-BSA. The amount of b-PG bound to the plate was then determined by the addition of peroxidase-labeled streptavidin, followed by a substrate for peroxidase.

2. In the next step, hyaluronan is released from the samples by digesting them overnight with trypsin or pronase (0.5 mg/mL, 37°C), which is then inactivated by heating to 100°C for 20 min. These samples, as well as a standard containing a known amount of hyaluronan, are serially diluted with PBS-A (100 µL per dilution).
3. An equal volume of 1 or 4 µg/mL b-PG in 10% calf serum, 90% PBS-A is added to each dilution and mixed for 1 h. Duplicate 50 µL aliquots of each dilution are then added to the wells of the 96-well plates that had been precoated with HA-BSA as described earlier. After shaking for 1 h, the plates are thoroughly washed with water and then incubated for 20 min with 100 µL/well of peroxidase labeled streptavidin diluted 1–500 in 10% calf serum, 90% PBS-A.
4. The plates are again washed with water and then to each well is added 100 µL of a peroxidase substrate consisting of 0.03% H_2O_2, 0.5 mg/mL 2,2' azinobis (3-ethylbenzthiazoline sulfonic acid) in 0.1 *M* Na citrate pH 4.2. After 30 min, the reaction is terminated by the addition of 25 µL/well of 2 m*M* NaN_3. The OD_{405} is determined using an ELISA reader.
5. When the OD_{405} of the standard is then plotted on semi-log paper, the curve is linear over the range from 50 ng/mL to 1 µg/mL of hyaluronan (*see* **Fig. 1**). Reading from test samples should be restricted to this central linear region. Control experiments showed that 10 µg/mL of chondroitin sulfate and heparin had little or no effect on the binding of b-PG to the plate.

4. Notes

1. The use of a Buchner funnel greatly facilitates the processing of the Sepharose. To transfer the gel from the funnel to a beaker, first allows the buffer to flow into the gel, release the vacuum, then rim the wall of the funnel with a spatula to separate the gel from the edge. Reapply the vacuum until the gel shrinks on top of the filter paper. The funnel is inverted and gel can be held as the filter paper is removed.

2. In some cases, we omit this lyophilization step, which saves a considerable amount of time. In this case, the appropriate amount of solid Hepes and Na acetate is added directly to the dialyzed extract.
3. To collect the b-PG in a minimal amount of buffer, it is important to keep a sharp interface with the guanidine buffer eluting the gel. To accomplish this, allow the 3 *M* NaCl to run into the top of the gel and then apply the 4 *M* guanidine to the top of the gel by inverting a 10-mL pipet so that the large opening is on the bottom.
4. Freeze thawing of the b-PG preparation in the absence of glycerol leads to a significant loss of binding activity.
5. Several factors influence the staining of hyaluronan with b-PG. First, the b-PG will only stain hyaluronan that is available to it. For this reason, the hyaluronan in cartilage does not stain because it is already complexed with proteins. Second, the hyaluronan may be lost from the section. When the synovial cavity is stained histochemically, no staining is observed because the hyaluronan is lost from the section.

Acknowledgment

This work was supported by the USAMRMC under grant number DAMD17-94-J-4173.

References

1. Green, S. J., Tarone, G., and Underhill, C. B. (1988) Distribution of hyaluronate and hyaluronate receptors in the adult lung. *J. Cell Sci.* **89,** 145–156.
2. Underhill, C. B., Nguyen, H. A., Shizari, M., and Culty, M. (1993) CD44 positive macrophages take up hyaluronan during lung development. *Dev. Biol.* **155,** 324–336.
3. Knudson, C. B. and Toole, B. P. (1985) Fluorescent morphological probe for hyaluronate. *J. Cell Biol.* **100,** 1753–1758.
4. Ripellino, J. A., Klinger, M. M., Margolis, R. U., and Morgolis, R. K. (1985) The hyaluronic acid binding region as a specific probe for the localization of hyaluronic acid in tissue sections. *J. Histochem. Cytochem.* **33,** 1060–1066.
5. Tengblad, A. (1979) Affinity chromatography on immobilized hyaluronate and its application to the isolation of hyaluronate binding proteins from cartilage. *Biochim. Biophys. Acta* **578,** 281–289.
6. Cambiaso, C. L., Goffinet, A., Vaerman, J.-P., and Heremans, J. F. (1975) Glutaraldehyde-activated aminohexyl-derivative of Sepharose as a new versatile immunoadsorbent. *Immunochemistry* **12,** 273–278.
7. Lin, W., Shuster, S., Maibach, H. I., and Stern, R. (1997) Patterns of hyaluronan staining are modified by fixation techniques. *J. Histochem. Cytochem.* **45,** 1157–1163.
8. Kusakabe, M., Sakakura, T., Nishizuka, Y., Sano, M., and Matsukage, A. (1984) A polyester wax embedding and sectioning technique for immunohistochemistry. *Stain Technol.* **59,** 127–132.
9. Graham, R. C., Lundholm, U., and Karnovsky, M. J. (1965) Cytochemical demonstration of peroxidase activity with 3-amino-9-ethyl carbazole. *J. Histochem. Cytochem.* **13,** 150–158.

[CANCER RESEARCH 61, 2434–2438, March 15, 2001]

Advances in Brief

RGD-Tachyplesin Inhibits Tumor Growth[1]

Yixin Chen, Xueming Xu, Shuigen Hong, Jinguo Chen, Ningfei Liu, Charles B. Underhill, Karen Creswell, and Lurong Zhang[2]

Department of Oncology, Lombardi Cancer Center, Georgetown University Medical School, Washington, D.C. 20007 [X-M. X., J. C., N. F., C. B. U., K. C., L. Z.], and The Key Laboratory of China Education Ministry on Cell Biology and Tumor Cell Engineering, Xiamen University, Fujian 361005, People's Republic of China [Y. C., S. H.]

Abstract

Tachyplesin is an antimicrobial peptide present in leukocytes of the horseshoe crab (*Tachypleus tridentatus*). In this study, a synthetic tachyplesin conjugated to the integrin homing domain RGD was tested for antitumor activity. The *in vitro* results showed that RGD-tachyplesin inhibited the proliferation of both cultured tumor and endothelial cells and reduced the colony formation of TSU prostate cancer cells. Staining with fluorescent probes of FITC-annexin V, JC-1, YO-PRO-1, and FITC-dextran indicated that RGD-tachyplesin could induce apoptosis in both tumor and endothelial cells. Western blotting showed that treatment of cells with RGD-tachyplesin could activate caspase 9, caspase 8, and caspase 3 and increase the expression of the Fas ligand, Fas-associated death domain, caspase 7, and caspase 6, suggesting that apoptotic molecules related to both mitochondrial and Fas-dependent pathways are involved in the induction of apoptosis. The *in vivo* studies indicated that the RGD-tachyplesin could inhibit the growth of tumors on the chorioallantoic membranes of chicken embryos and in syngenic mice.

Introduction

Tachyplesin, a peptide from hemocytes of the horseshoe crab (*Tachypleus tridentatus*), can rapidly inhibit the growth of both Gram-negative and -positive bacteria at extremely low concentrations (1, 2). Tachyplesin has a unique structure, consisting of 17 amino acids (KWCFRVCYRGICYRRCR) with a molecular weight of 2,269 and a pI of 9.93. In addition, it contains two disulfide linkages, which causes all six of the basic amino acids (R, arginine; K, lysine) to be exposed on its surface (3). The cationic nature of tachyplesin allows it to interact with anionic phospholipids present in the bacterial membrane and thereby disrupt membrane function (4, 5).

The structural nature of tachyplesin suggested that it might also possess antitumor properties. Tachyplesin can interact with the neutral lipids in the plasma membrane of eukaryotic cells (4, 5). More importantly, because it can interact with the membranes of prokaryotic cells, it is likely that tachyplesin can also interact with the mitochondrial membrane of eukaryotic cells. Indeed, these membranes are structurally similar because mitochondria are widely believed to have evolved from prokaryotic cells that have established a symbiotic relationship with the primitive eukaryotic cell (6). Recent studies have indicated that mitochondria play a critical role in regulating apoptosis in eukaryotic cells (7). The disruption of mitochondrial function results in the release of proteins that normally are sequestered by this organelle. The release of factors, such as cytochrome *c* and Samc, can activate caspases that, in turn, trigger the apoptotic cascade (8, 9). Along these lines, Ellerby *et al.* (10) have found that a cationic antimicrobial peptide (KLAKLAKKLAKLAK) conjugated with a CNGRC homing domain exhibits antitumor activity through its ability to target mitochondria and trigger apoptosis. Because the proapoptotic peptide and tachyplesin belong to the same category of cationic antimicrobial peptide, it seems possible that tachyplesin could have similar antitumor activity.

To explore this possibility, we have examined a chemically synthesized preparation of tachyplesin that was linked to a RGD sequence, which corresponds to a homing domain that allows it to bind to integrins on both tumor and endothelial cells and thereby facilitates internalization of the peptide (11, 12). We found that this synthetic RGD-tachyplesin could inhibit the proliferation of TSU prostate cancer cells and B16 melanoma cells as well as endothelial cells in a dose-dependent manner *in vitro* and reduce tumor growth *in vivo*.

Materials and Methods

Synthesis of RGD-Tachyplesin. Two peptides were chemically synthesized. The test peptide was RGD-tachyplesin (CRGDCGGKWCFRVCYRGICYRRCR), and the control peptide was a scrambled sequence with a similar molecular weight and pI. To impede enzymatic degradation, the NH_2-terminal of the peptide was acetylated, and the COOH-terminal was amidated. Before use, the peptides were dissolved in dimethylformamide and 1% acetate acid, diluted with saline to a concentration of 1 mg/ml, and sterilized by boiling for 15 min in a water bath.

Cell Lines. The TSU human prostate cancer cells, B16 melanoma, Cos-7, and NIH-3T3 were maintained in 10% calf serum and 90% DMEM. The human umbilical vein endothelial cells and ABAE[3] cells were cultured in 20% fetal bovine serum and 80% DMEM containing 10 ng/ml fibroblast growth factor 2 and vascular endothelial growth factor, respectively.

Cell Proliferation Assay. Aliquots of complete medium containing 5000 cells were distributed into a 96-well tissue culture plate. The next day, the media were replaced with 160 μl of fresh media and 40 μl of a solution containing different concentrations of the peptides. One day later, 30 μl of 0.3 μCi of [^{3}H]thymidine in serum-free media were added to each well, and after 8 h, the cells were harvested, and the amount of incorporated [^{3}H]thymidine was determined with a beta counter.

Colony Formation Assay. TSU cells (2×10^4) were suspended in 1 ml of 0.36% agarose in 90% DMEM and 10% calf serum containing 100 μg/ml control peptide or RGD-tachyplesin and then immediately placed on the top of a layer of 0.6% solid agarose in 10% calf serum and 90% DMEM in 6-well plates. Two weeks later, the number of colonies larger than 60 μm in diameter was determined using an Omnicon Image Analysis system (Imaging Products International Inc., Chantilly, VA).

Analysis of Tachyplesin-damaged Cells by Flow Cytometry. Cultures of TSU cells at 80% confluence were treated overnight with 50 μg/ml control peptide or RGD-tachyplesin. The next day, the cells were harvested with 5 mM EDTA in PBS, washed, resuspended in 10% calf serum and 90% DMEM, and then stained with the fluorescent dyes annexin V and propidium iodide, JC-1,

Received 11/22/00; accepted 1/30/01.

The costs of publication of this article were defrayed in part by the payment of page charges. This article must therefore be hereby marked *advertisement* in accordance with 18 U.S.C. Section 1734 solely to indicate this fact.

[1] Supported in part by National Cancer Institute/NIH Grant R29 CA71545; United States Army Medical Research and Materiel Command Grants DAMD17-99-1-9031, DAMD17-98-1-8099, DAMD17-00-1-0081, and PC970502; and Susan G. Komen Breast Cancer Foundation (C. B. U. and L. Z.). Y. C. was a recipient of China Scholarship Council, and L. Z. was a recipient of funding from the visiting scholar foundation for key laboratory at Xiamen University, China.

[2] To whom requests for reprints should be addressed. at Department of Oncology, Lombardi Cancer Center Georgetown University Medical School, 3970 Reservoir Road, NW, Washington, D.C. 20007. Phone: (202) 687-6397; Fax: (202) 687-7505; E-mail: Zhangl@georgetown.edu.

[3] The abbreviations used are: ABAE, adult bovine aorta endothelial; FADD, Fas-associated death domain; CAM, chorioallantoic membrane.

YO-PRO-1, and FITC-dextran, according to manufacturer's instructions (Molecular Probes, Eugene, OR).

Western Blotting. Cultures of TSU and ABAE cells at approximately 80% confluence were treated overnight with 100 μg/ml peptides and then harvested with 1 ml of lysis buffer (1% Triton X-100, 0.5% sodium deoxycholate, 0.5 μg/ml leupetin, 1 mM EDTA, 1 μg/ml pepstatin, and 0.2 mM phenylmethylsulfonyl fluoride). The protein concentration was determined by the BCA method (Pierce, Rockford IL), and 20 μg of protein lysate were loaded onto 4–12% BT NuPAGE gel (Invitrogen, Carlsbad CA), electrophoresed, and transferred to a nitrocellulose membrane. The loading and transfer of equal amounts of protein were confirmed by staining with Ponceau S solution (Sigma, St. Louis, MO). The membranes were blocked with 5% nonfat milk and 1% polyvinylpyrrolidone in PBS for 30 min and then incubated for 1 h with 1 μg/ml antibodies to Fas ligand, FADD, caspase 9, caspase 8, caspase 3, caspase 7, and caspase 6 (Oncogene, Boston, MA). After washing, the membrane was incubated for 1 h with 0.2 μg/ml of peroxidase-labeled antirabbit IgG followed by a chemiluminescent substrate for peroxidase and exposed to enhanced chemiluminescence Hyperfilm MP (Amersham, Piscataway, NJ).

Effect of RGD-Tachyplesin on TSU Tumor Growth on the Chicken CAM. TSU cells (2×10^6) were mixed with equal amounts of control peptide or RGD-tachyplesin (100 μg in 200 μl of saline) and immediately placed on top of the CAMs of 10-day-old chicken embryos (15 eggs/group) and incubated at 37.8°C. Every other day thereafter, 200 μl of PBS containing 100 μg of the peptides were added tropically to the xenografts on the CAMs. Five days later, the xenografts were dissected from the membrane, photographed, and weighed.

Effect of RGD-Tachyplesin on B16 Tumor Growth in Mice. B16 melanoma cells were injected s.c. into the flank of 5-week-old male C57BL/6 mice (5×10^5 cells/site; 5 mice/group) and allowed to establish themselves for 2 days. Every other day thereafter, 250 μg of the control peptide or RGD-tachyplesin was injected i.p. into the mice. At the end of 2 weeks, the mice were sacrificed, and the tumor xenografts were removed, photographed, and weighed.

Statistical Analysis. The mean and SE were calculated from the raw data and then subjected to Student's t test. $P < 0.05$ was regarded as statistical significance.

Results

RGD-Tachyplesin Inhibits the Growth of Tumor and Endothelial Cells *in Vitro*. Because both tumor and endothelial cells play an important role in determining tumor progression, we initially examined the effects of RGD-tachyplesin on the proliferation of both of these cells *in vitro*. As shown in Fig. 1*A*, RGD-tachyplesin inhibited the growth of the cultured cells in a dose-dependent manner, with an EC_{50} of about 75 μg/ml for TSU tumor cells and 35 μg/ml for the endothelial cells. In contrast, the scrambled peptide had no obvious effect on the proliferation of the cells at 100 μg/ml. This effect was also reflected in the morphology of the cells. After exposure to 50 μg/ml RGD-tachyplesin for 12 h, a significant fraction of treated cells had become rounded and detached, whereas few cells did so after treatment with the control peptide (data not shown).

To determine whether nontumorigenic cells were also affected by RGD-tachyplesin, the immortalized cell lines, Cos-7 and NIH-3T3, were tested in the [^{3}H]thymidine incorporation assay. As shown in Fig. 1*B*, when treated with 50 μg/ml RGD-tachyplesin, the extent of inhibition of Cos-7 or NIH-3T3 (0–20%) was less than that of tumor or proliferating endothelial cells (40–75%), indicating that nontumorigenic cells are less sensitive to RGD-tachyplesin.

Next, we examined the effects of the peptides on the growth of TSU cells in soft agar. The ability of cells to grow under such anchorage-independent conditions is one of the characteristic phenotypes of aggressive tumor cells. As shown in Fig. 1*C*, RGD-tachyplesin inhibited the ability of TSU cells to form colonies as compared to the groups of control peptide and vehicle alone.

Treatment with RGD-Tachyplesin Alters Membrane Function. We then examined the mechanism by which RGD-tachyplesin inhibited the proliferation of the tumor and endothelial cells. One possibility was that RGD-tachyplesin damages cell membranes, and this damage, in turn, induces apoptosis.

To examine the extent of apoptosis, TSU cells that had been treated for 1 day with the test or control peptides were stained with FITC-annexin and propidium iodide. FITC-annexin V binds to phosphatidylserine, which is exposed on the outer leaflet of the plasma membrane of cells in the initial stages of apoptosis, whereas propidium iodide preferentially stains the nucleus of dead cells, but not living cells. Fig. 2*A* shows that treatment with RGD-tachyplesin induced apoptosis (annexin V positive, propidium iodide negative) in a greater number of cells than did treatment with the vehicle or control peptide.

This induction of apoptosis could have been due to the disruption of mitochondrial function. To examine this, we used JC-1 staining, which measures the membrane potential of mitochondria. As shown in Fig. 2, *B* and *C*, treatment with RGD-tachyplesin caused a shift in the fluorescence profile from one that was highly red (Fig. 2*B*) to one that was less red and more green (Fig. 2*C*). This indicated that the membrane potential of mitochondria was changed by treatment with RGD-tachyplesin.

We also examined the integrity of the plasma membrane and nuclear membrane after treatment with the scrambled peptide and RGD-tachyplesin using two different fluorescent markers. YO-PRO-1 dye can only stain the nuclei of cells with damaged plasma and nuclear membranes. Fig. 2*D* shows that treatment with RGD-tachyplesin allowed the YO-PRO-1 dye to pass into the nuclei, causing an increase in the fluorescence intensity. Similar results were obtained when the cells were stained with FITC-dextran, which is not taken up by viable, healthy cells but can pass through the damaged plasma membrane of unhealthy cells. Fig. 2*E* shows that cells treated with RGD-tachyplesin took up a greater amount of FITC-dextran (M_r 40,000) than did those treated with the control peptide. These results indicated that the majority of RGD-tachyplesin-treated cells allowed these big molecules to pass their damaged membranes.

The above-mentioned experiments were also carried out with ABAE cells, and similar results were obtained (data not shown). Presumably, RGD-tachyplesin induces apoptosis in both TSU and ABAE cells by damaging their membranes.

RGD-Tachyplesin Triggers Apoptotic Pathways. Apoptosis can be induced by two mechanisms: (*a*) the mitochondrial pathway; and (*b*) the death receptor pathway (13). To identify the nature of the apoptotic pathway triggered by RGD-tachyplesin, both TSU and ABAE cells were treated overnight with RGD-tachyplesin and control peptide and then analyzed by Western blotting for the alterations of molecules involved in the mitochondrial and Fas-dependent pathways. Fig. 3 shows that treatment of both TSU tumor cells and ABAE cells with RGD-tachyplesin caused the cleavage of M_r 46,000 caspase 9 into subunits of M_r 35,000 and M_r 10,000, indicating activation of the mitochondrial-related, Fas-independent pathway. In addition, RGD-tachyplesin treatment could up-regulate the expression of upstream molecules in the Fas-dependent pathway, including Fas ligand (M_r 43,000), FADD (M_r 28,000), and activate subunits of caspase 8 (M_r 18,000). Furthermore, the downstream effectors, such as caspase 3 subunits (M_r 20,000), caspase 6 (M_r 40,000), and caspase 7 (M_r 34,000), were also up-regulated by RGD-tachyplesin. These results suggest that RGD-tachyplesin induces apoptosis through both the mitochondrial-related, Fas-independent pathway and the Fas-dependent pathway. However, because there is cross-talk between these two pathways (13), we do not have enough evidence to determine which one is the initiator.

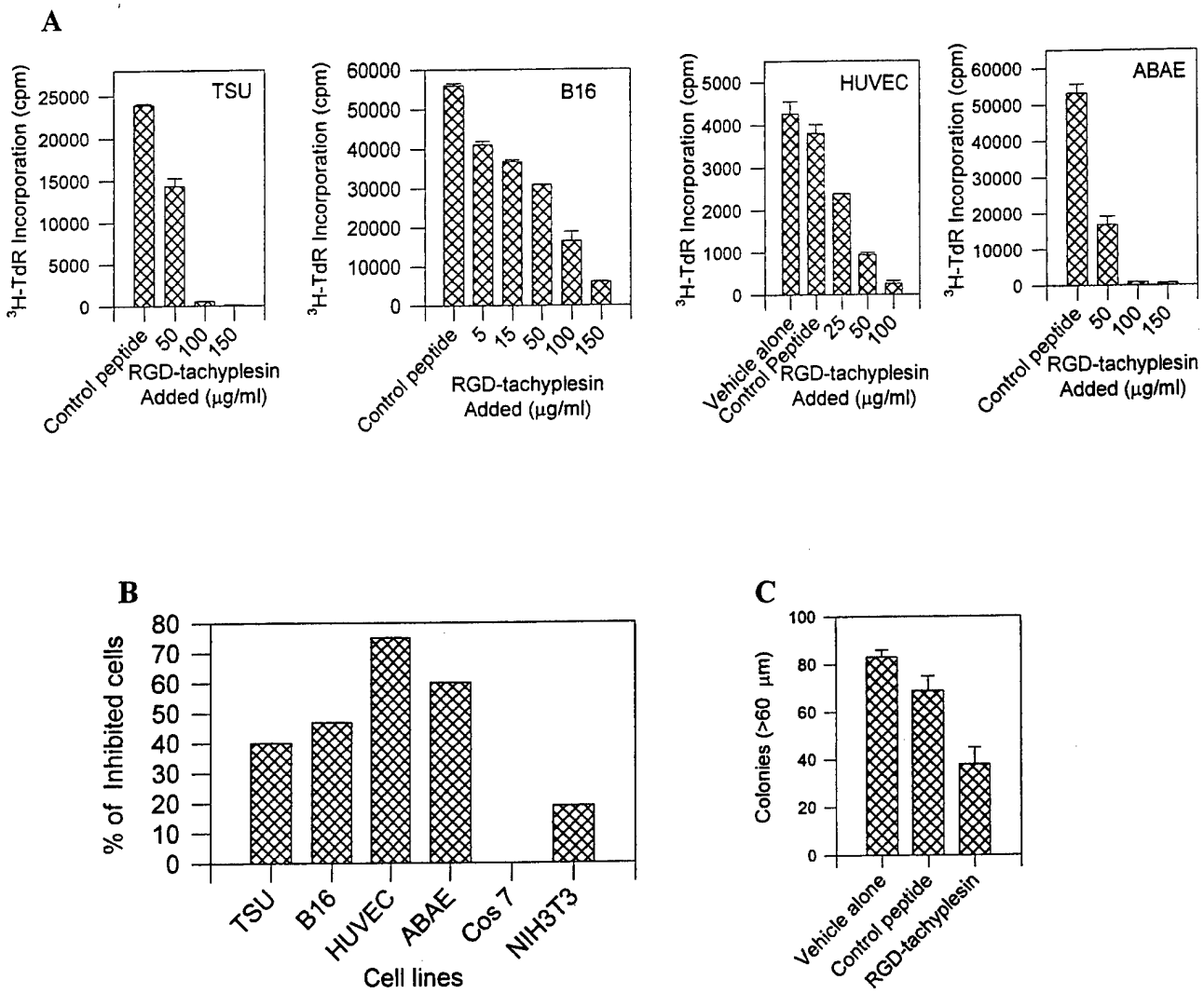

Fig. 1. Effects of RGD-tachyplesin and scrambled peptide on cell proliferation. *A*, effect of RGD-tachyplesin on cell proliferation. TSU cells were treated with vehicle alone, 100 μg/ml control peptide, or different doses of RGD-tachyplesin for 24 h, followed by a [^{3}H]thymidine incorporation assay. The proliferation of both the tumor and endothelial cells was greatly inhibited by RGD-tachyplesin in a dose-dependent manner ($P < 0.01$). *B*, effect of RGD-tachyplesin on different cell lines. The cells were treated overnight with 50 μg/ml control peptide or RGD-tachyplesin and then treated with [^{3}H]thymidine. The rate of inhibition was calculated as follows: (1 − cpm of cells treated with RGD-tachyplesin/cpm of cells treated with control peptide) × 100%. The nontumorigenic cell lines Cos-7 and NIH-3T3 were inhibited to a lesser degree than the tumor or endothelial cells ($P < 0.05$). *C*, effect of RGD-tachyplesin on colony formation of TSU cells. TSU cells were suspended in 0.36% agarose containing 100 μg/ml control peptide or RGD-tachyplesin and then placed on top of 0.6% agarose. Two weeks later, colonies larger than 60 μm were counted with the Omnicon Image Analysis system. The colony formation of TSU cells was inhibited by RGD-tachyplesin ($P < 0.01$). All of the experiments were repeated three times, and similar results were obtained.

RGD-Tachyplesin Inhibits the Growth of TSU and B16 Tumor *in Vivo*. In the final series of experiments, we examined the *in vivo* effects of RGD-tachyplesin on the growth of TSU or B16 tumor cells in CAM (14) or mouse models. As shown in Fig. 4, the TSU tumor xenografts growing in CAM in the group treated with RGD-tachyplesin (Fig. 4*B*) were smaller than those in the group treated with control peptide (Fig. 4*A*). In addition, the average weight of the xenografts in the RGD-tachyplesin-treated group was significantly less than that of xenografts in the control group (Fig. 4*C*). Similarly, in the B16 mouse model, the B16 tumor xenografts in the RGD-tachyplesin-treated group (Fig. 4*E*) were smaller than those in the control group (Fig. 4*D*), and this difference was statistically significant ($P < 0.05$; Fig. 4*F*). It should be noted that RGD-tachyplesin did not appear to be toxic to the mice, as judged by their weights and activity at the end of the experiment. Thus, the results from two models are consistent with each other, indicating that RGD-tachyplesin can inhibit tumor growth *in vivo*.

Discussion

The major conclusion of this study is that RGD-tachyplesin can inhibit tumor growth by inducing apoptosis in the tumor cells and the associated endothelial cells. This conclusion was supported by the following observations. First, RGD-tachyplesin was able to inhibit the growth of TSU tumor cells on the CAM of chicken embryos as well as the growth of B16 tumor cells in syngenic mice. Second, RGD-tachyplesin also blocked the proliferation of both tumor and endothelial cells in culture in a dose-dependent fashion, whereas proliferation was relatively unaffected in nontumorigenic cell lines Cos-7 and NIH-3T3. Third, RGD-tachyplesin induced apoptosis in cultured TSU cells, as indicated by staining with fluorescent markers for apoptosis including FITC-annexin V, which detects exposed phosphatidylserine, and JC-1, which tracks mitochondrial membrane potential. Finally, RGD-tachyplesin stimulated the activation and production of several molecules in the apoptotic cascade in both TSU and endothelial cells, as judged by Western blotting.

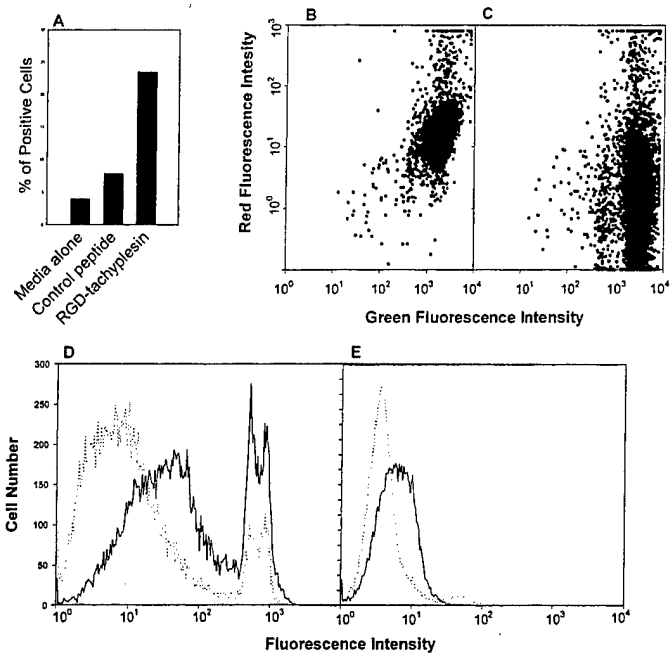

Fig. 2. The effect of RGD-tachyplesin on the function of TSU cells. TSU cells were treated overnight with 50 μg/ml control peptide or RGD-tachyplesin and then stained with different membrane probes. *A*, staining with annexin V and propidium iodide for apoptotic cells. The percentage of cells that were positive for FITC-annexin V and negative for propidium iodide was analyzed by flow cytometry. The RGD-tachyplesin-treated cells had a high percentage of apoptotic cells ($P < 0.01$). *B* and *C*, staining with JC-1 for mitochondrial membrane potential. The cells treated with the control peptide (*B*) and RGD-tachyplesin (*C*) were stained with 10 μg/ml JC-1 for 10 min and then analyzed by flow cytometry. The RGD-tachyplesin shifted the spectrum of the cells from high red (*B*, healthy) to high green and low red (*C*, loss mitochondrial potential). *D*, staining with YO-PRO-1 for integrity of nuclei membrane. The peptide-treated cells were stained with 0.1 μg/ml YO-PRO-1 dye, an indicator for damaged nuclei membranes (the *first peak* represents the dye-stained G_0-G_1-phase cells; the *second peak* represents the dye-stained S-M-phase cells). The RGD-tachyplesin treated cells shift from right to left, indicating the loss of integrity of the nuclei membrane. *E*, staining with FITC-dextran for integrity of plasma membrane. The peptide-treated cells were incubated with 50 μg/ml FITC-dextran (M_r 40,000) for 30 min and analyzed with flow cytometry. A higher proportion of RGD-tachyplesin-treated cells allowed FITC-dextran to pass through their plasma membrane as compared to the control.

Our results also suggest that RGD-tachyplesin up-regulates apoptosis related to both the mitochondrial and the death receptor pathways. The involvement of the mitochondrial pathway was suggested by the facts that staining with JC-1 indicated the membrane potential of mitochondria was decreased (Fig. 2, *B* and *C*) and that the caspase 9 was activated (Fig. 3) in cells treated with RGD-tachyplesin. Presumably, this resulted from the release of cytochrome *c*, which, in turn, bound to Apaf-1 and activated caspase 9 and then caspase 3, caspase 7, and caspase 6 (13, 15–17). This is the mechanism by which the peptide described by Ellerby *et al.* (10) induced apoptosis. In addition, we found that members of the death receptor pathway (Fas ligand, FADD, and caspase 8) were also up-regulated. Thus, RGD-tachyplesin may have multiple effects on the target cells. It is difficult at this point to determine what initial event is responsible for the RGD-tachyplesin-induced activation of apoptosis.

There appears to be considerable cross-talk between the mitochondrial apoptotic pathway and Fas-dependent pathway. The caspase 6 activated by the mitochondrial pathway (cytochrome *c*→Apaf-1→caspase 9→caspase 3) could act on FADD and then on caspase-8, which triggered the Fas-dependent pathway. On the other hand, the caspase 8-activated Fas-FADD pathway could act on BID that stimulates the mitochondrial pathway (15–17). This cross-talk creates positive feedback and enhances the apoptosis cascade.

RDG-tachyplesin also appeared to be relatively nontoxic to cells not associated with tumors. When RGD-tachyplesin was administered at a concentration that inhibited tumor growth, there was no notable side effects on either the chicken embryos or mice with regard to animal body weight and activity at the end of each experiment. In addition, studies on cultured cells indicated that the sensitivity to RGD-tachyplesin varied depending on cell type. In comparison to tumor cells and proliferating endothelial cells, immortalized cells such as Cos-7 (green monkey kidney cells) and NIH-3T3 (fibroblast cells) were less sensitive to RGD-tachyplesin. Taken together, these results suggest that RGD-tachyplesin is a well-tolerated peptide.

RGD-tachyplesin also appears to be more potent than similar cationic peptides. The unique cyclic structure of tachyplesin maintained by two disulfide bonds may make it more effective in targeting membranes than the linear antimicrobial peptides, such as KLAK-LAKKLAKLAK (a proapoptotic peptide; Ref. 10), which is suggested by its lower minimal inhibition concentration on both *Escherichia coli* and *Staphylococcus aureus* of 2 *versus* 6 μM (18, 19). Furthermore, tachyplesin interacts not only with anionic phospholipids of bacterial and mitochondria but also with neutral lipids of eukaryotic plasma membrane (4, 5, 18). Ellerby *et al.* (10) reported that their proapoptotic peptide inhibited proliferation with an EC_{50} of about 100 μg/ml for endothelial cells, whereas our results indicated that RGD-tachyplesin had a much stronger efficacy on proliferating

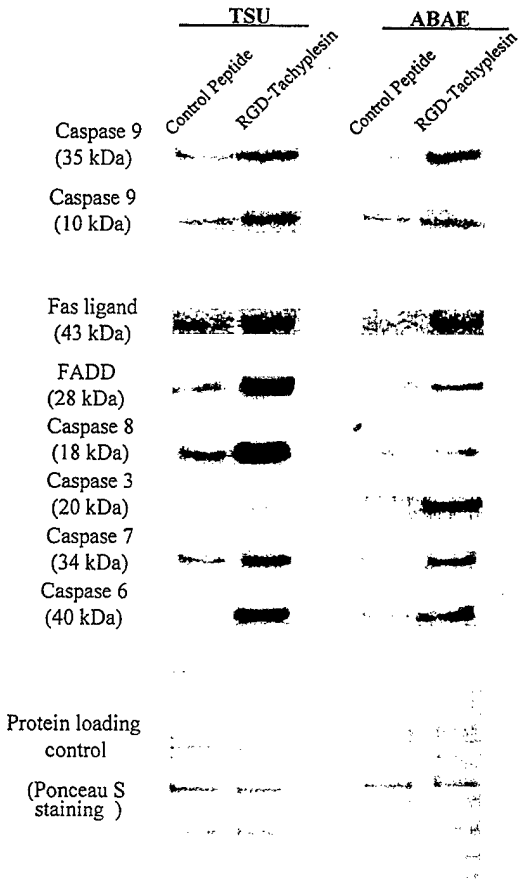

Fig. 3. Effect of RGD-tachyplesin on molecules involved in the apoptosis cascade. Twenty μg of lysate from TSU and ABAE cells treated with 100 μg/ml control peptide or RGD-tachyplesin were loaded onto a 4–12% BT NuPAGE gel, electrophoresed, and transferred to a nitrocellulose membrane. The loading and transfer of equal amounts of protein were confirmed by staining with a Ponceau S solution. After blocking with 5% nonfat milk, the membranes were incubated for 1 h with 1 μg/ml antibodies to caspase 9, Fas ligand, FADD, caspase 8, caspase 3, caspase 7, and caspase 6 followed by horseradish peroxidase-conjugated antirabbit IgG and enhanced chemiluminescence substrate and finally exposed to Hyperfilm MP.

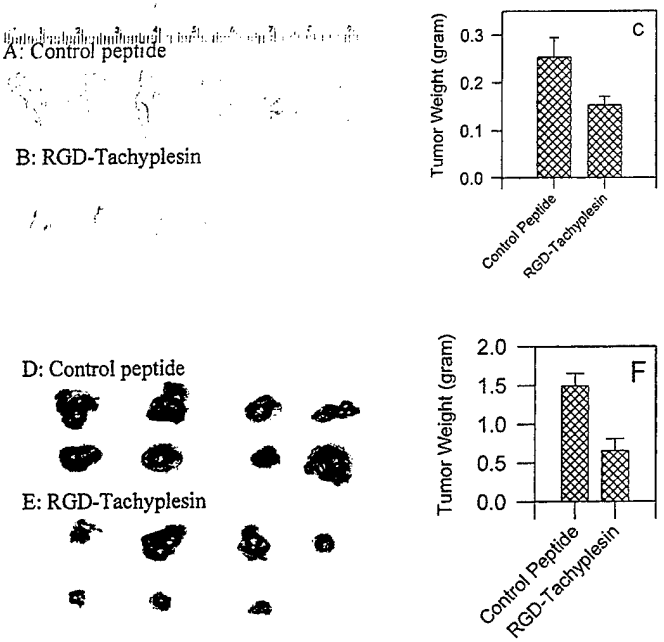

Fig. 4. Effect of RGD-tachyplesin on tumor growth *in vivo*. *A–C*, effect of RGD-tachyplesin on the TSU xenografts on CAM. TSU cells (2×10^6) were mixed with either control peptide or RGD-tachyplesin (100 μg) and immediately placed on top of the CAM of 10-day-old chicken embryos and incubated at 37.8°C. Every other day, additional peptides were applied tropically to the TSU xenografts. Five days later, the xenografts were removed from the CAM, photographed, and weighed. The TSU xenografts treated with RGD-tachyplesin were significantly smaller than those treated with the control peptide ($P < 0.01$). *D–F*, effect of RGD-tachyplesin on tumor growth in the mouse model. B16 melanoma cells (5×10^5) were injected s.c. into the flank of C57BL/6 mice and allowed to establish themselves for 2 days. Every other day after that, 250 μg of control peptide or RGD-tachyplesin were injected i.p. into the mice. At the end of 2 weeks, the mice were sacrificed, and the xenografts were removed, photographed, and weighed. The B16 xenografts from animals treated with RGD-tachyplesin were significantly smaller than those from animals treated with the control peptide ($P < 0.01$).

endothelial cells, with an EC_{50} of about 35 μg/ml. Furthermore, RGD-tachyplesin acts not only on proliferating endothelial cells but also on tumor cells. This dual effect of RGD-tachyplesin will enhance its antitumor function.

In conclusion, this study demonstrates that RGD-tachyplesin can be used as an antitumor agent. By disrupting vital membranes and inducing apoptosis, it inhibits all of the tumor cells tested. Further study of RGD-tachyplesin and its analogues may lead to finding a new category of antitumor drug.

Acknowledgments

The animal protocols were reviewed and approved by the Animal Care and Use Committee of Georgetown University.

References

1. Kokryakov, V. N., Harwig, S. S., Panyutich, E. A., Shevchenko, A. A., Aleshina, G. M., Shamova, O. V., Korneva, H. A., and Lehrer, R. I. Protegrins. Leukocyte anti-microbial peptides that combine features of corticostatic defensins and tachyplesins. FEBS Lett., *327:* 231–236, 1993.
2. Shigenaga, T., Muta. T., Toh, Y., Tokunaga, F., and Iwanaga. S. Anti-microbial tachyplesin peptide precursor. cDNA cloning and cellular localization in the horseshoe crab (*Tachypleus tridentatus*). J. Biol. Chem., *265:* 21350–21354, 1990.
3. Nakamura. T., Furunaka, H., Miyata, T., Tokunaga. F., Muta, T., Iwanaga, S., Niwa. M., Takao, T., and Shimonishi, Y. Tachyplesin, a class of anti-microbial peptide from the hemocytes of the horseshoe crab (*Tachypleus tridentatus*). Isolation and chemical structure. J. Biol. Chem., *263:* 16709–16713, 1988.
4. Park. N. G., Lee, S., Oishi, O., Aoyagi, H., Iwanaga, S., Yamashita, S., and Ohno, M. Conformation of tachyplesin I from *Tachypleus tridentatus* when interacting with lipid matrices. Biochemistry, *31:* 12241–12247, 1992.
5. Katsu, T., Nakao, S., and Iwanaga, S. Mode of action of an anti-microbial peptide, tachyplesin I, on biomembranes. Biol. Pharm. Bull., *16:* 178–181, 1993.
6. Gray, M. W., Burger, G., and Lang. B. F. Mitochondrial evolution. Science (Washington DC), *283:* 1476–1481, 1999.
7. Brenner, C., and Kroemer, G. Mitochondria: the death signal integrators. Science (Washington DC), *289:* 1150–1151, 2000.
8. Li, H., Kolluri, S. K., Gu, J., Dawson, M. I., Cao, X., Hobbs, P. D., Lin, B., Chen, G., Lu, J., Lin, F., Xie, Z., Fontana, J. A., Reed, J. C., and Zhang, X. Cytochrome *c* release and apoptosis induced by mitochondrial targeting of nuclear orphan receptor TR3. Science (Washington DC), *289:* 1159–1164, 2000.
9. Du, C., Fang, M., Li, Y., Li, L., and Wang, X. Smac, a mitochondrial protein that promotes cytochrome *c*-dependent caspase activation by eliminating IAP inhibition. Cell, *102:* 33–42, 2000.
10. Ellerby, H. M., Arap, W., Ellerby, L. M., Kain, R., Andrusiak, R., Rio, G. D., Krajewski, S., Lombardo, C. R., Rao, R., Ruoslahti, E., Bredesen, D. E., and Pasqualini, R. Anti-cancer activity of targeted pro-apoptotic peptides. Nat. Med., *5:* 1032–1038, 1999.
11. Arap, W., Pasqualini, R., and Ruoslahti, E. Cancer treatment by targeted drug delivery to tumor vasculature in a mouse model. Science (Washington DC), *279:* 377–380, 1998.
12. Brooks, P. C., Clark, R. A. F., and Cheresh, D. A. Requirement of vascular integrin $\alpha_v\beta_3$ for angiogenesis. Science (Washington DC), *264:* 569–571, 1994.
13. Kaufmann, S. H., and Earnshaw, W. C. Induction of apoptosis by cancer chemotherapy. Exp. Cell Res., *256:* 42–49, 2000.
14. Brooks, P. C., Silletti, S., von Schalscha, T. L., Friedlander, M., and Cheresh, D. A. Disruption of angiogenesis by PEX, a noncatalytic metalloproteinase fragment with integrin binding activity. Cell, *92:* 391–400, 1998.
15. Liu, X., Kim, C. N., Yang, J., Jemmerson, R., and Wang, X. Induction of apoptotic program in cell-free extracts: requirement for dATP and cytochrome *c*. Cell, *86:* 147–157, 1996.
16. Desagher, S., Osen-Sand, A., Nichols, A., Eskes, R., Montessuit, S., Lauper, S., Maundrell, K., Antonsson, A., and Martinou, J. C. Bid-induced conformational change of Bax is responsible for mitochondrial cytochrome *c* release during apoptosis. J. Cell Biol., *144:* 891–901, 1999.
17. Slee, E. A., Harte, M. T., Kluck, R. M., Wolf, B. B., Casiano, C. A., Newmeyer, D. D., Wang, H-G. Reed, J. C., Nicholson, D. W., Alnemri, E. S., Green, D. R., and Martin, S. J. Ordering the cytochrome *c*-initiated caspase cascade: hierarchical activation of caspases-2, -3, -7, -8, and -10 in a caspase-9-dependent manner. J. Cell Biol., *144:* 281–292, 1999.
18. Matsuzaki, K. Why and how are peptide-lipid interactions utilized for self-defense? Magainins and tachyplesins as archetypes. Biochim. Biophys. Acta, *1462:* 1–10, 1999.
19. Javadpour, M. M., Juban, M. M., Lo, W. C., Bishop, S. M., Alberty, J. B., Cowell, S. M., Becker, C. L., and McLaughlin, M. L. *De novo* anti-microbial peptides with low mammalian cell toxicity. J. Med. Chem., *39:* 3107–3113, 1996.